

1-23-92
E-6519

Detailed Noise Measurements on the SR-7A Propeller: Tone Behavior With Helical Tip Mach Number

James H. Dittmar
National Aeronautics and Space Administration
Lewis Research Center
Cleveland, Ohio

and

David G. Hall
Sverdrup Technology, Inc.
Lewis Research Center Group
Brook Park, Ohio

December 1991



DETAILED NOISE MEASUREMENTS ON THE SR-7A PROPELLER:

TONE BEHAVIOR WITH HELICAL TIP MACH NUMBER

James H. Dittmar
National Aeronautics and Space Administration
Lewis Research Center
Cleveland, Ohio 44135

and

David G. Hall
Sverdrup Technology, Inc.
Lewis Research Center Group
Brook Park, Ohio 44142

SUMMARY

Detailed noise measurements were taken on the SR-7A propeller to investigate the behavior of the noise with helical tip Mach number. Data sets taken at constant advance ratio and at constant axial Mach number both showed the noise to first rise with increasing helical tip Mach number and then to level off as the Mach number was increased further. This behavior was further investigated by obtaining detailed pressure-time histories of the data. The pressure-time histories indicate that a portion of the primary pressure pulse is progressively canceled by a secondary pulse which results in the noise leveling off as the helical tip Mach number is increased. This second pulse appears to originate on the same blade as the primary pulse and is in some way connected to the blade itself. This leaves open the possibility of redesigning the blade to improve the cancellation and thereby reduce the propeller noise.

INTRODUCTION

Advanced turboprop-powered aircraft offer the potential for significant fuel savings over equivalent core technology turbofan-powered aircraft. The noise from advanced high speed propellers at cruise conditions is of present concern since it may pose a problem in the airplane cabin. A number of model propellers have previously been tested for acoustics in the NASA Lewis Research Center's 8- by 6-Foot Wind Tunnel (ref. 1 to 6). In this previous testing it was observed that the maximum blade passing tone first rises with increasing helical tip Mach number then levels off or decreases as the helical tip Mach number is further increased. An understanding of this noise behavior is desirable for reducing noise at cruise. To further investigate this behavior, detailed noise measurements were made on the SR-7A propeller during the Swirl Recovery Vane test program and some preliminary results were presented in reference 7. The data obtained here were collected at more closely spaced operating conditions than had been tested previously (refs. 1 to 6) and the measurements were subject to more detailed analysis. This report presents the results of these experiments and the detailed analysis of the data.

APPARATUS AND PROCEDURE

The SR-7A propeller, which is nominally 62.2 cm (24.5 in.) in diameter was tested for acoustics in the NASA Lewis 8- by 6-Foot Wind Tunnel. Table I shows some of the design

characteristics of this propeller. A plan view of the wind tunnel is shown in figure 1(a) and a photograph of the SR-7A propeller in the test section is shown in figure 1(b). Previous data taken on this propeller were reported in reference 6. The propeller was tested here at the test conditions presented in Table II and shown in figure 2. Data were taken at a constant advance ratio of 3.06 for closely spaced Mach numbers (circles in fig. 2) and at closely spaced advance ratios for constant Mach numbers of $M = 0.85$ (triangles), $M = 0.8$ (squares), $M = 0.75$ (diamonds) and $M = 0.7$ (pentagons). The highest available test rig rotative speed limited the lowest advance ratios that were possible at $M = 0.8$ to 2.84 and at $M = 0.85$ to 3.0 and limited the highest axial Mach number that could be tested at an advance ratio of 3.06 to 0.86. For these experiments the propeller was operated at its nominal design blade setting angle, measured at $3/4$ radius, of 60.1° .

A plate was mounted from the tunnel ceiling, 0.3 propeller diameters from the tip, and transducers were installed flush with the plate surface to measure the noise of the propeller. A photograph of this plate is shown in figure 3(a) and a sketch of the plate is shown in figure 3(b). Twelve transducers were installed on the plate centerline, which was directly above the propeller centerline. The transducer locations are shown in figure 3(b). The signals from the pressure transducers were recorded on magnetic tape and narrowband, frequency domain, spectra were obtained for each of the test points. Typically the narrowband range was 0 to 10 000 Hz with a bandwidth of 32 Hz. However, because the propeller blade passing frequency was so close to the wind tunnel compressor tones at some of the test conditions, some higher resolution spectra (0 to 2500 Hz with a 8 Hz bandwidth) were performed to isolate the propeller tone.

In addition, the data were reduced to pressure-time histories by using signal enhancement with a once per revolution signal as a trigger (synchronous time averaging). This enhancement was necessary to obtain propeller only time histories because of the high level of the tunnel compressor tones and the tunnel background noise.

RESULTS AND DISCUSSION

Noise Variation With Helical Tip Mach Number

Variation at constant advance ratio of 3.06. - As observed in figure 2, a series of tests at a constant advance ratio of 3.06 was performed at various axial Mach numbers from 0.6 to 0.86 (horizontal line of circles in fig. 2). At constant advance ratio, the variation in axial Mach number provides the variation in helical tip Mach number. The maximum sideline tone levels observed for the first three blade passing frequency harmonics are plotted versus helical tip Mach number in figure 4.

The maximum blade passing tone variation from these data is plotted versus helical tip Mach number in figure 4(a) along with previous data on this propeller taken from reference 6. The two sets of data show good general agreement. The previous data are presented here because they go to a higher helical tip Mach number than the present data. As can be observed in figure 4(a) the noise first rises with helical tip Mach number then levels off around a helical tip Mach number $M_{ht} = 1.15$ and slightly decreases to a local minima around $M_{ht} = 1.21$ and then starts to rise again. The previous data point from reference 6 is the one that shows the rise at the higher helical tip Mach number. The design operating point of this propeller is around the $M_{ht} = 1.15$ condition which is the noisiest point on the curve. This curve indicates that a

blade passing tone noise decrease is possible if the propeller were to be designed to operate near the minimum noise point of $M_{ht} = 1.21$.

Figures 4(b) and (c) show the noise variation with helical tip Mach number of the tone at twice and three times blade passing frequency, respectively. They show the same general behavior as the blade passing tone having first a noise increase with increasing helical tip Mach number, then a levelling off to a local minima and finally a noise increase again. The leveling off for the harmonics occurs at a lower helical tip Mach number than for the blade passing tone. The tone at twice blade passing frequency starts to level off at $M_{ht} = 1.1$ and the tone at three times blade passing frequency starts to level off at $M_{ht} = 1.05$. As the helical tip Mach number is further increased both harmonics start to rise again at a lower helical tip Mach number than did the blade passing tone. This behavior is noted here and will be discussed further in the pressure-time history sections later in this report.

Variations at constant advance ratios of 3.6, 3.4, and 3.2. - The variations of the maximum blade passing tone with helical tip Mach number for constant advance ratios of 3.6, 3.4, and 3.2 are plotted in figure 5. The variation in helical tip Mach number is provided by testing at varying axial Mach number with the constant advance ratio (see fig. 2). As can be seen in figure 5 the noise at constant advance ratio first rises with increasing helical tip Mach number and then levels off. The local minima and the subsequent rise that were observed at a constant advance ratio of 3.06 are not observed here assumedly because the data were not taken at high enough helical tip Mach numbers.

Variation at constant axial Mach number. - Data were taken at constant axial Mach number and the advance ratio was varied to obtain the variation in helical tip Mach number. These are the vertical lines of symbols on figure 2. The variation of maximum blade passing tone with helical tip Mach number, taken at axial Mach numbers of 0.85, 0.80, 0.75, and 0.70 are shown in figure 6. The curves at axial Mach numbers of 0.85 and 0.80, figures 6(a) and (b), show the noise rise with increasing helical tip Mach number and the levelling off at the higher helical tip Mach numbers. The curve at an axial Mach number of 0.75 (fig. 6(c)), is a straight line and does not show a levelling off. The data at an axial Mach number of 0.7 also shows a straight line (fig. 6(d)). The lack of levelling off for these curves is assumedly because data were not taken at a high enough helical tip Mach number.

The presence of the levelling off for the data taken at constant axial Mach number as well as at constant advance ratio, indicates that a quieter propeller could be designed by taking advantage of this behavior of the noise with helical tip Mach number. An understanding of this noise behavior is then desirable and a more detailed analysis of the pressure-time histories of the data is presented in the following sections.

Pressure - Time Histories

Histories at $M = 0.8$, $J = 3.06$. - Pressure-time histories were obtained by signal enhancement using a once per revolution signal from the propeller (synchronous time averaging). The individual transducers were not phase calibrated with respect to one another, so any differences in phase seen on the pressure time traces has no physical significance. Figure 7 shows the pressure-time histories for the twelve transducer positions on the acoustic plate when the propeller was operating at an axial Mach number of 0.8 and an advance ratio of 3.06. Each of the figures shows slightly more than the 360° of a revolution. The first two positions, 1 and 2, do

not show much activity and indicate that even with signal enhancement the propeller noise signature is below the broadband level. At the farther aft positions the signals from each of the eight blades can be seen. The peak blade passing tone level was obtained at both transducers 7 and 8. It is interesting to note that even with the somewhat different pulse shapes the blade passing tone levels were the same at these two positions. Each of these traces represents an average of approximately 40 propeller revolutions.

Histories at constant advance ratio of 3.06.- As indicated previously in figure 4, the noise first rises with increasing helical tip Mach number and then levels off as the helical tip Mach number is further increased. Pressure-time histories were taken at the maximum blade passing tone location for axial Mach numbers of 0.72, 0.80, 0.82, 0.84, and 0.86 with a constant advance ratio of 3.06 and are presented in figure 8. The analysis of this set of pressure-time histories gives us some understanding of what is causing the noise versus helical tip Mach number curve to level off.

The pressure-time history of figure 8(a) is at an axial Mach number of 0.72 which yields a helical tip Mach number of 1.03 at the constant advance ratio of 3.06. Referring to figure 4(a) it can be seen that this pressure-time history is taken on a portion of the curve where the noise is still rising with increasing helical tip Mach number. The figure shows one pulse from each of the eight blades. The pulse consists of a broad positive portion and a sharp negative portion. This negative portion is larger in magnitude than the positive portion and is a major contributor to the blade passing tone.

As the helical tip Mach number is increased to the peak blade passing tone noise level on figure 4(a) ($M = 0.8$, $M_{ht} = 1.14$), the pressure-time history of figure 8(b) is observed. This pressure-time history is very similar in shape to the one at $M = 0.72$, $M_{ht} = 1.03$, having a broad and slightly larger positive pulse and a sharp negative portion. However, the negative portion of the pulse is showing the presence of a second positive pulse which is starting to fill in the negative portion. This is highlighted by the arrows in figure 8(b). The exact shape of this additional pulse is not known. Here it appears to be a single hump but at higher Mach numbers, as will be shown later, it appears to have more than one hump. The filling in of the negative portion of the pulse is starting to limit the growth of the blade passing tone with increasing helical tip Mach number.

As the helical tip Mach number is further increased the secondary pulse grows in strength (fig. 8(c)), $M = 0.82$, $M_{ht} = 1.17$, until it starts to show up both in the positive portion of the initial pulse as well as the negative portion, figures 8(d) and (e) at $M_{ht} = 1.20$ and $M_{ht} = 1.23$ respectively. On figure 8(e), $M = 0.86$, $M_{ht} = 1.23$, the second pulse has partially filled the trough and is showing up as a second spike on the positive portion. It appears that this second pulse, with its canceling interference on the primary pulse, is the reason the peak blade passing tone does not continue to increase with helical tip Mach number.

Since the higher harmonics of the blade passing tone are controlled even more than the blade passing tone by the sharp negative portion of the curve, the secondary pulse has a more immediate effect on their noise behavior. As noted before (figs. 4(a) and (b)), the higher harmonics start to show a levelling off in the noise curve at a lower helical tip Mach number. The secondary pulse causes a smoothing in the sharp negative portion of the trace (fig. 8(b)) and results in the higher harmonics being affected sooner. At the higher helical tip Mach numbers, the harmonics start their noise rise at a lower helical tip Mach number than the blade passing tone. This can be seen in the pressure-time history of figure 8(e). At this condition, the blade

passing tone has not yet started to rise (fig. 4(a)) but the tone at twice blade passing frequency has started to increase (fig. 4(b)). When looking at the two positive pressure pulses for each blade on figure 8(e) it would appear that this would contribute most to the fourth harmonic since that is the approximate spacing of the second pulse. The additional noise at the second harmonic is quite possibly the result of this second positive spike also. Because of the importance in determining the noise behavior with helical tip Mach number, an understanding of the source of the second pulse is desirable.

During this testing to obtain pressure-time waveforms, one of the eight propeller blades had a shortened chord at the tip. This was the result of some previous damage to the blade. Figure 9(a) shows a normal blade and figure 9(b) shows the trailing edge region of the shortened chord blade. The result of this shortened chord blade tip can be seen in the pressure-time history of figure 8(e). The last pulse on these traces is believed to be from the blade with the shortened tip chord. As can be seen from figure 8(e), the blade with the shortened tip chord has a smaller primary pressure-time signature than the other blades. This indicates, that at these conditions, the blade tip region is the controlling noise producing region of the blade. It can also be observed that the strength of the secondary pulse is reduced even more than the initial pulse, indicating that the second pulse is from the same blade as the initial pulse.

One of the possible sources considered for the secondary pulse was a reflection of an initial pulse from some other surface, such as the tunnel walls, the propeller hub, or another propeller blade. An examination of the trace in figure 8(e) shows that the second pulse from the shortened blade is arriving behind the initial pulse by about one-fourth of the spacing between the two blades. This one-fourth blade spacing distance would then have to be the distance between the direct and reflected path lengths. In viewing the geometry, the noise path lengths to any of the possible reflecting surfaces are much larger than the distance between the primary and secondary pulses. The possibility of a direct reflection during the same revolution of the propeller is then eliminated. For the secondary pulse to be a reflection of the shortened blades primary pulse, the reflection would then have to be arriving some whole number of revolutions of the propeller later than the initial pulse and falling back onto the same initial blade pressure pulse. Although this scenario is theoretically possible for some specific propeller speed and transducer location, the timing of the reflected pulse would vary with a change in propeller speed or transducer position and the reflected pulse would fall someplace else in the pressure-time history. The data at other propeller speeds and other transducer locations shows the same relative timing of the initial and secondary pulses. For example, figure 10 shows the pressure-time histories for transducers 7 to 9 at $M = 0.86$, $M_{ht} = 1.23$. As can be seen the eighth blade shows the reduced primary and secondary pulses at all three transducer locations and the secondary pulse trails the initial pulse by the same amount at each position. This then eliminates the possibility that the secondary pulse is a reflection of the initial pulse from the shortened blade. Reference 7 showed a pressure-time history from the SR-3 propeller tested in flight on the Jetstar airplane which also showed the secondary pulse filling in the initial pulse just as it does on the SR-7A propeller. This figure is repeated here as figure 11. The presence of this interfering pulse on a different propeller in a different type of test facility showed that the phenomena is not unique to the 8- by 6-foot wind tunnel or to the SR-7A propeller.

The secondary pulse is then indicated as originating on the same propeller blade as the initial pulse. The spike type nature of the secondary pulse shape is similar to that for a shock wave and may be from a trailing edge shock on the blade. The secondary pulse could also be the result of the blade spanwise loading or thickness distribution. In any case, the secondary pulse is related directly to the blade and it may be possible to improve on this cancellation or shift it to

another Mach number range if desired. To do this, however, will require a deeper understanding of the secondary pulse source.

Histories at constant Mach number of 0.8. - Figure 12 shows the pressure-time histories taken at a constant axial Mach number of 0.8 with advance ratios varying in steps of 0.1 from 3.5 to 2.9. Figure 12(a), $J = 3.5$ represents the lowest helical tip Mach number at 1.07. Here the trace exhibits a pulse with a broad positive portion and a sharp negative portion. As the helical tip Mach number is increased the secondary pulse starts to appear (fig. 12(c), $J = 3.3$, $M_{ht} = 1.10$). The secondary pulse grows in strength and is seen most strongly at the highest helical tip Mach numbers in figures 12(e), to (g). In the blade passing tone versus helical tip Mach number at constant Mach number of 0.8 (fig. 6(b)), it is these last three highest Mach numbers where the curve starts to bend over. The presence of this secondary pulse is then seen as the cause of the levelling off of the noise curve for data taken at constant Mach number as well as at constant advance ratio.

CONCLUDING REMARKS

Detailed noise measurements were taken on the SR-7A propeller to investigate the behavior of the noise with helical tip Mach number. Data taken with constant advance ratio, varying axial Mach number, showed the maximum blade passing tone to first rise with helical tip Mach number then level off reaching a local minima and then increase again. This behavior pattern also existed for the maximum tones at twice and three times blade passing frequency. Here, at the harmonics, the tone levelled off at a lower helical tip Mach number and started back up again at a lower helical tip Mach number than did the tone at blade passing frequency. Data were also taken at constant axial Mach numbers of 0.8 and 0.85 with varying advance ratio. Here the noise rose with increasing helical tip Mach number and then began to level off as did the curves at constant advance ratio. Data taken at constant axial Mach numbers of 0.75 and 0.70 showed only a straight line increase with increasing helical tip Mach number presumably because they did not reach a high enough helical tip Mach number to show the flattening of the curve.

The presence of the levelling off for the noise versus helical tip Mach number curve at both constant advance ratio and constant axial Mach number indicates that a quieter propeller could be designed by taking advantage of this behavior. Further analysis of this behavior was undertaken by obtaining detailed pressure-time histories of the data. The pressure-time histories were obtained by signal enhancement using a once per revolution signal (synchronous time averaging).

The pressure-time histories at the low helical tip Mach numbers, those on the increasing portion of the maximum noise versus helical tip Mach number curves, showed one pulse per blade. These pulses consisted of a broad positive pulse and a sharp negative pulse. The negative portion was larger in magnitude than the positive portion and constituted a major contribution to the blade passing tone and its harmonics.

As the helical tip Mach number was increased to where the blade passing tone versus helical tip Mach number curve starts to level off, the negative portion of the history starts to show the presence of a second positive pulse. This second positive pulse is filling in the negative portion of the pulse and limits the growth of the blade passing tone with increasing helical tip Mach number. The higher harmonics of the blade passing tone are affected earlier by this filling

in of the negative portion because this sharp negative portion is apparently more directly controlling the level of the harmonics. The second positive pulse appears to originate on the same blade as the initial pulse and is in some way connected to the blade itself. This leaves open the possibility of redesigning the blade to improve this cancellation and thereby achieving a quieter propeller.

REFERENCES

1. Dittmar, J.H.; Jeracki, R.J.; and Blaha, B.J.: Tone Noise of Three Supersonic Helical Tip Speed Propellers in a Wind Tunnel. NASA TM-79167, 1979.
2. Dittmar, J.H.; and Jeracki, R.J.: Additional Noise Data on the SR-3 Propeller. NASA TM-81736, 1981.
3. Dittmar, J.H.; Stefko, G.L.; and Jeracki, R.J.: Noise of the 10-Bladed 60° Swept SR-5 Propeller in a Wind Tunnel. NASA TM-83054, 1983.
4. Dittmar, J.H.: Preliminary Measurement of the Noise from the 2/9 Scale Model of the Large-Scale Advanced Propfan (LAP) Propeller, SR-7A. NASA TM-87116, 1985.
5. Dittmar, J.H.: Cruise Noise of the SR-2 Propeller Model in a Wind Tunnel. NASA TM-101480, 1989.
6. Dittmar, J.H.; and Stang, D.B.: Cruise Noise of the 2/9th Scale Model of the Large-Scale Advanced Propfan (LAP) Propeller, SR-7A. NASA TM-100175, 1987.
7. Dittmar, J.H.; and Hall, D.G.: The Effect of Swirl Recovery Vanes on the Cruise Noise of an Advanced Propeller. NASA TM-103625, AIAA Paper 90-3932, 1990.

TABLE I. - SR-7A PROPELLER DESIGN CHARACTERISTICS

Diameter, cm(in.)	62.2 (24.5)
Number of blades	8
Design Mach number	0.80
Design speed, m/sec (ft/sec)	244 (800)
Design advance ratio	3.06
Design power coefficient	1.45
Design power loading, kW/m ² (hp/ft ²)	257 (32.0)
Integrated design lift coefficient	0.202
Activity factor	227
Design efficiency, percent	79

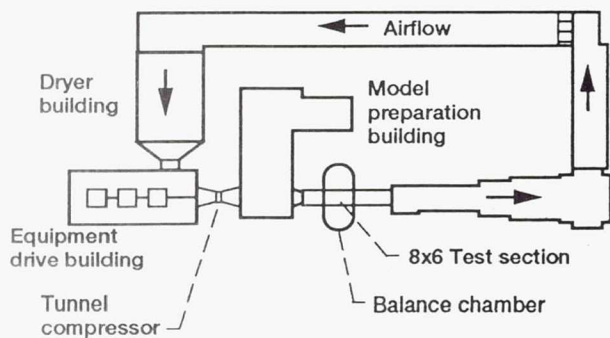
TABLE II. - PROPELLER TEST
CONDITIONS

(a) Tests at constant advance
ratio of 3.06

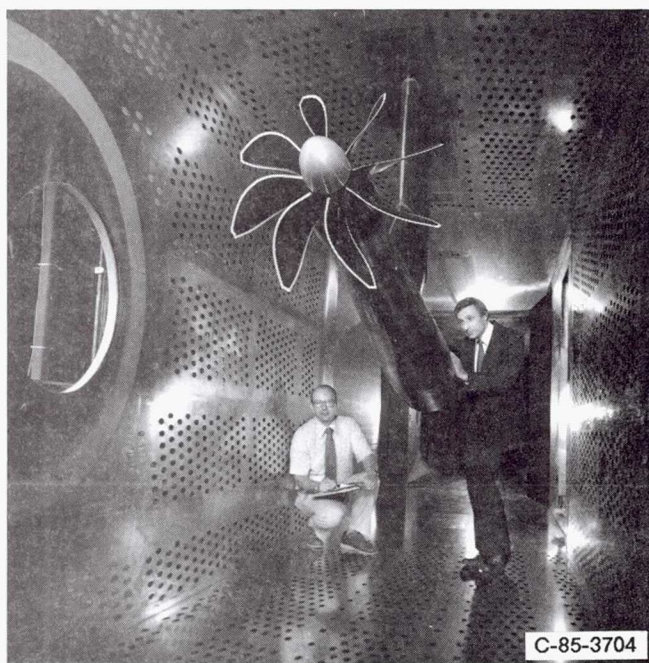
Axial Mach number	Advance ratio	Helical tip Mach number
0.6	3.06	0.857
.65	↓	.932
.7		1.001
.72		1.030
.74		1.059
.75		1.074
.76		1.090
.78		1.117
.8		1.146
.82		1.175
.84		1.201
.85		1.215
.86		1.230

(b) Tests at constant axial
Mach number

Axial Mach number	Advance ratio	Helical tip Mach number
0.8	3.8	1.039
	3.7	1.049
	3.6	1.062
	3.5	1.072
	3.4	1.086
	3.3	1.101
	3.2	1.116
	3.1	1.132
	3.0	1.158
	2.9	1.176
.85	2.84	1.188
	3.8	1.103
	3.6	1.131
	3.4	1.157
	3.2	1.189
.75	3.0	1.223
	3.8	.972
	3.6	.994
	3.4	1.019
	3.2	1.051
	3.0	1.084
.7	2.8	1.128
	3.8	.910
	3.6	.927
	3.4	.951
	3.2	.976
	3.0	1.013
	2.8	1.049



(a) Plan view of NASA Lewis 8- by 6-foot wind tunnel.



(b) SR-7A in test section.

Figure 1.—Wind tunnel and propeller installation.

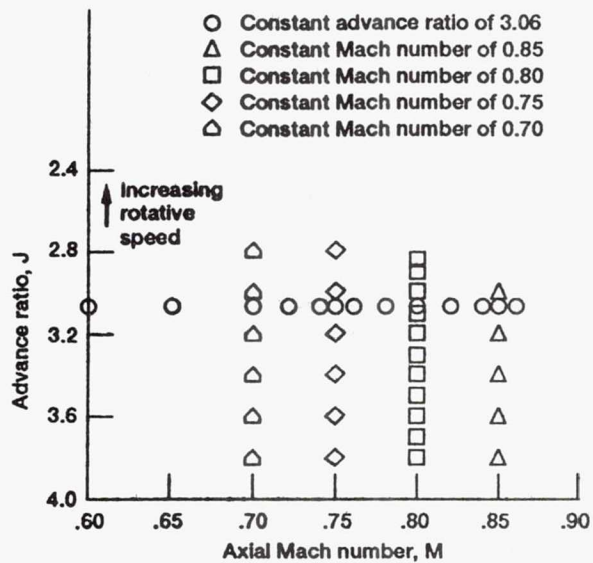
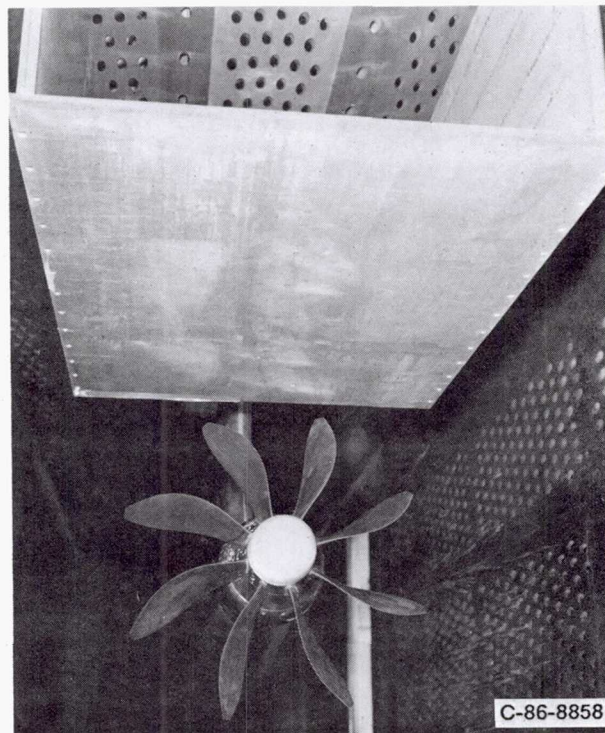
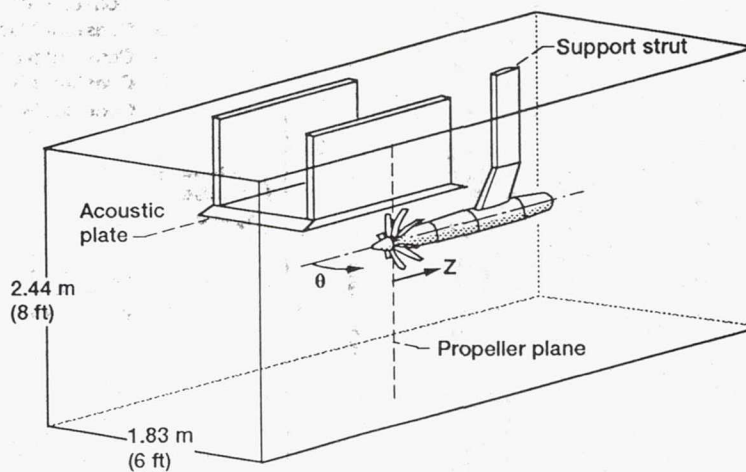


Figure 2.—Advance ratio and axial Mach number of experimental data points.



(a) Photograph.



Position	Transducer (plate 0.3 diameter from tip)											
	1	2	3	4	5	6	7	8	9	10	11	12
Transducer position, cm (in.)												
Z	-46.7 (-18.4)	-41.7 (-16.4)	-30.5 (-12.0)	-16.0 (-6.3)	-8.9 (-3.5)	0.8 (0.3)	8.9 (3.5)	12.4 (4.9)	18.0 (7.1)	25.0 (9.9)	28.7 (11.3)	42.4 (16.7)
Angle from upstream, deg												
0	46.8	50.0	58.5	72.2	80	90.9	100	104	110	116.8	120	130.4

(b) Transducer locations.

Figure 3.—Acoustic plate.

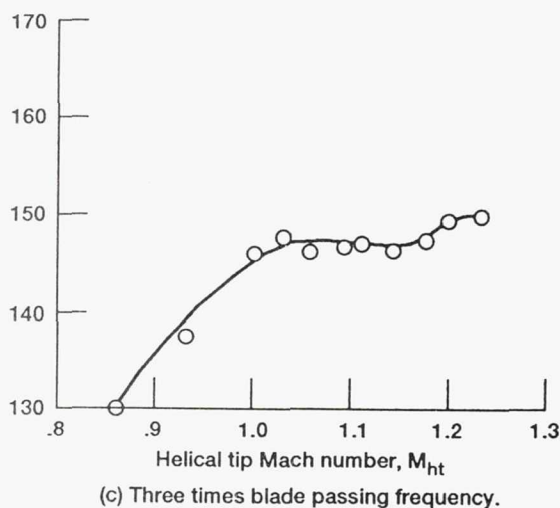
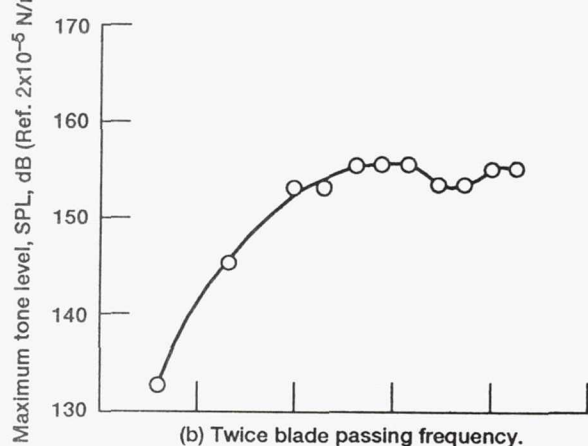
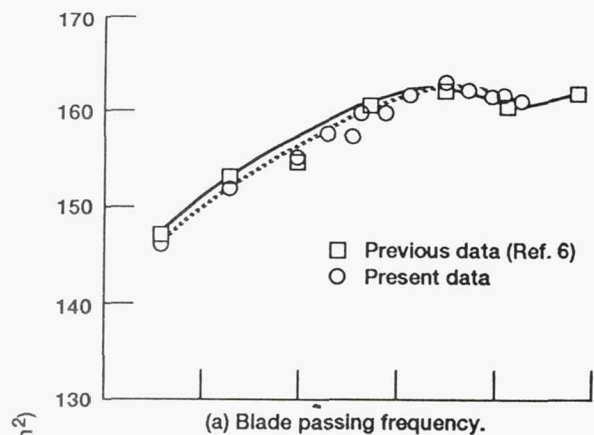


Figure 4.—Maximum tone versus helical tip Mach number at constant advance ratio of 3.06.

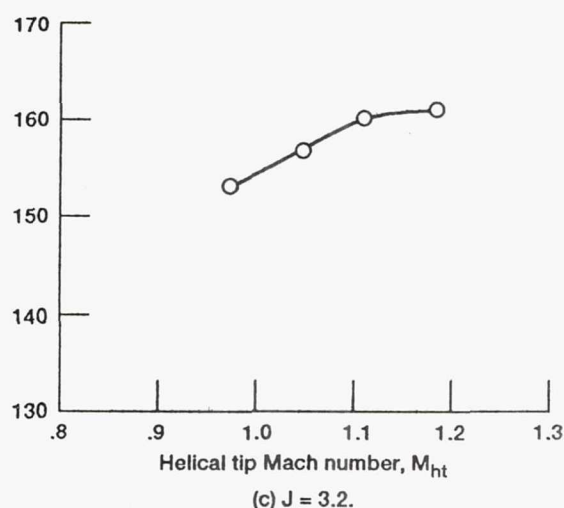
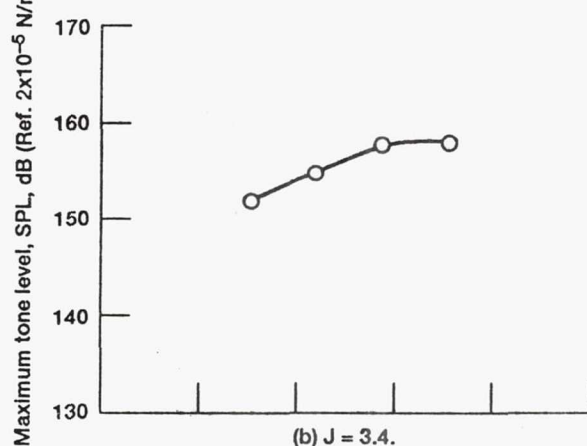
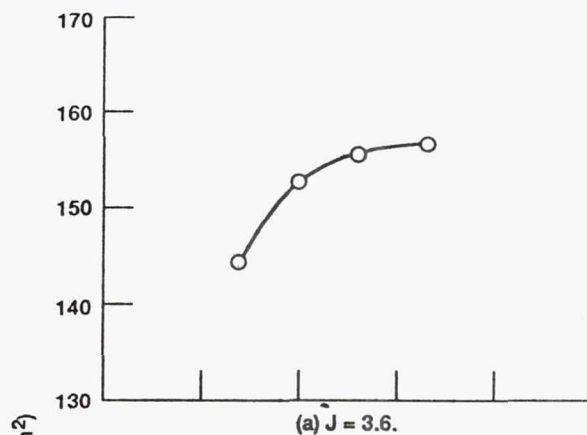


Figure 5.—Maximum blade passing tone versus helical tip Mach number at constant advance ratio.

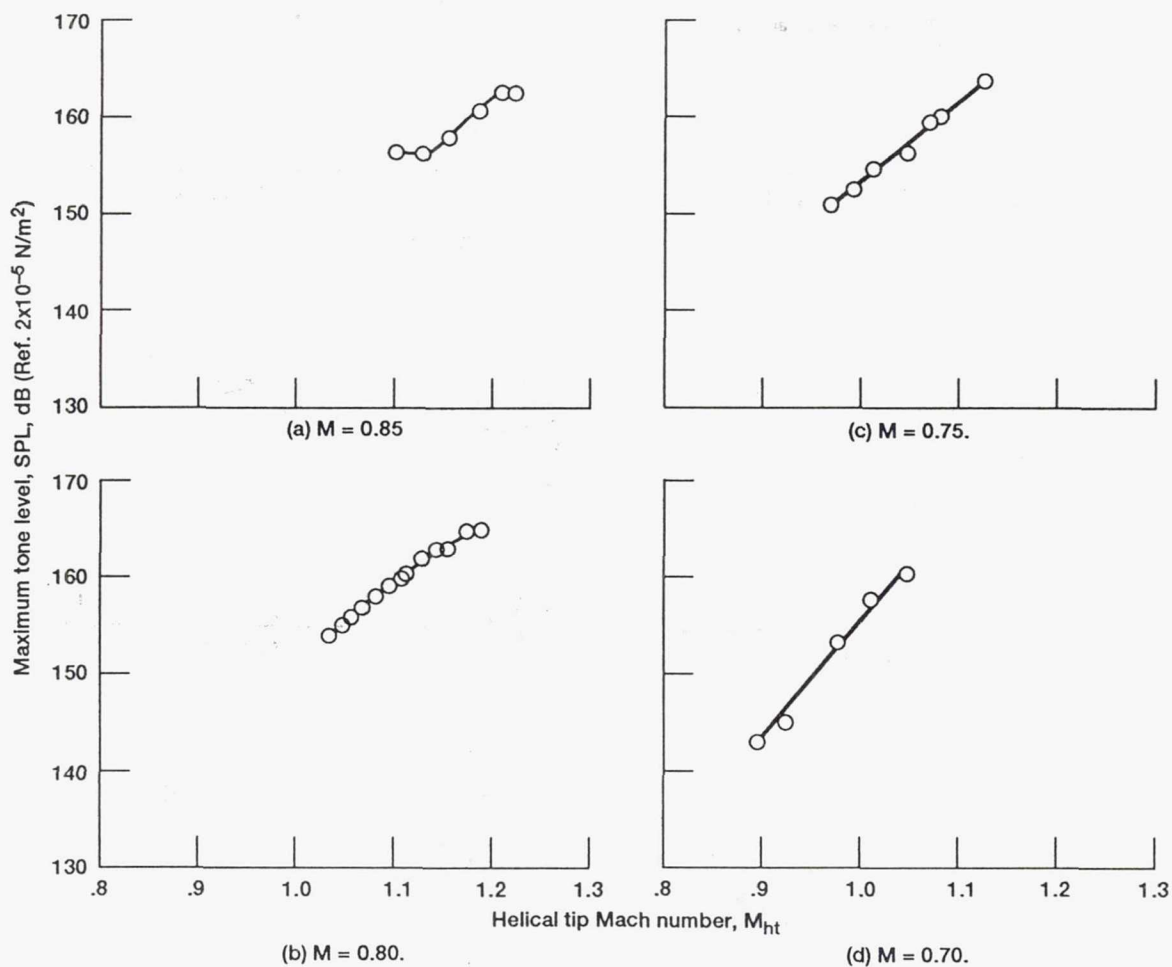
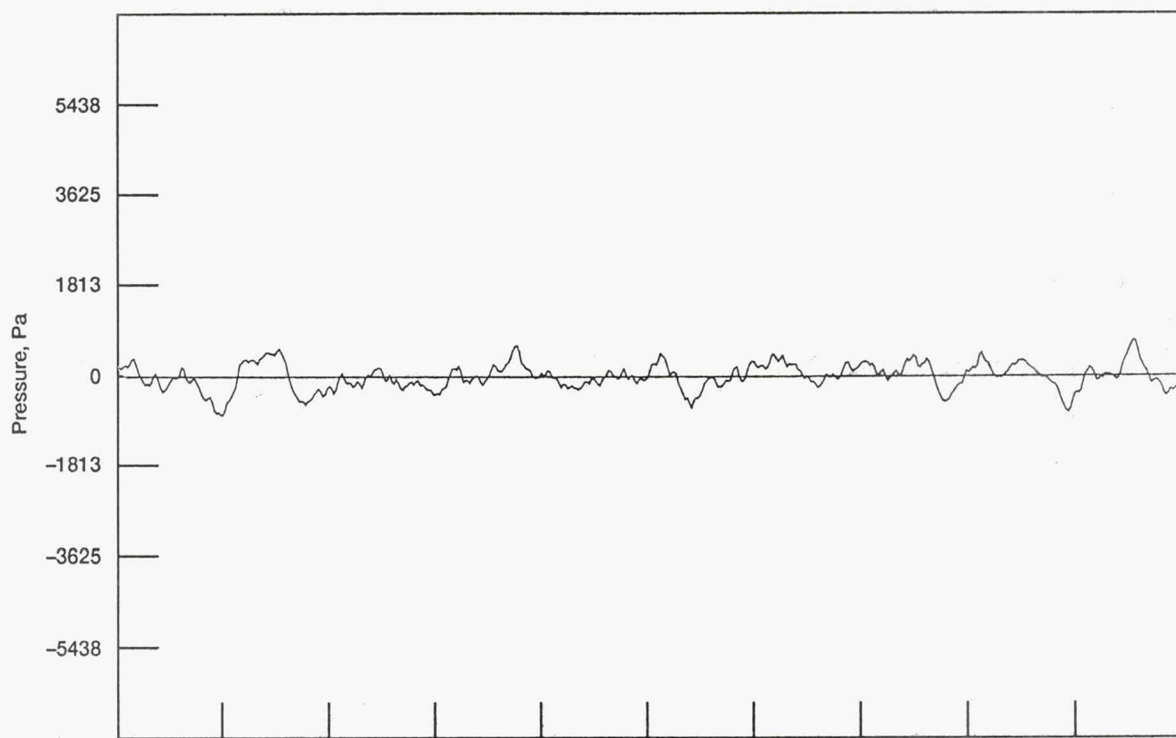
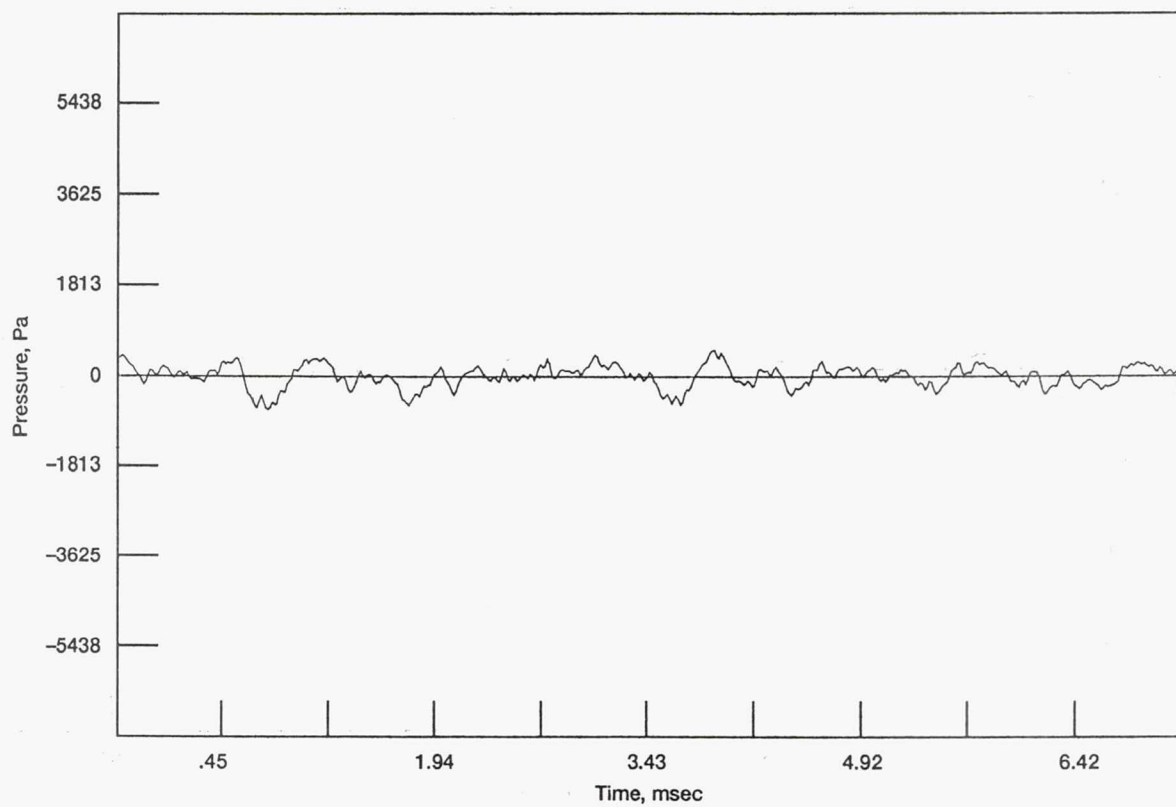


Figure 6.—Maximum blade passing tone versus helical tip Mach number at constant axial Mach number.

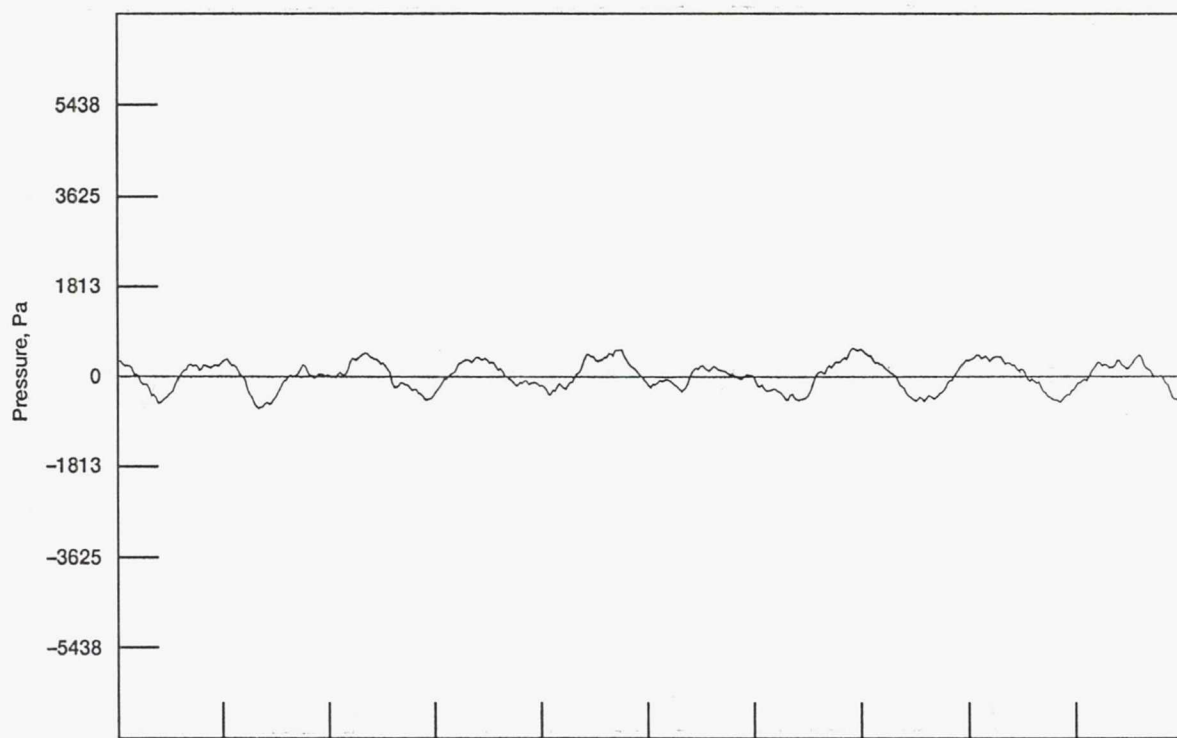


(a) Transducer 1.

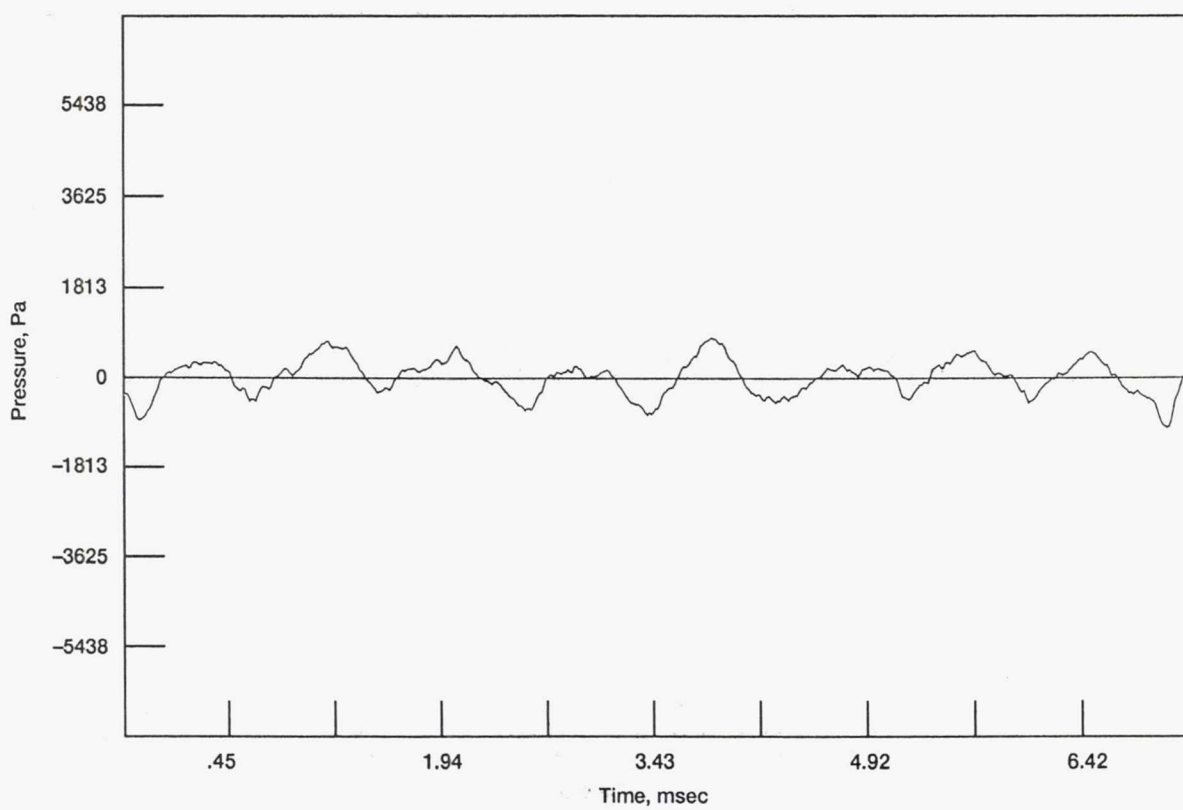


(b) Transducer 2.

Figure 7.—Pressure time histories at $M = 0.8$, $J = 3.06$.

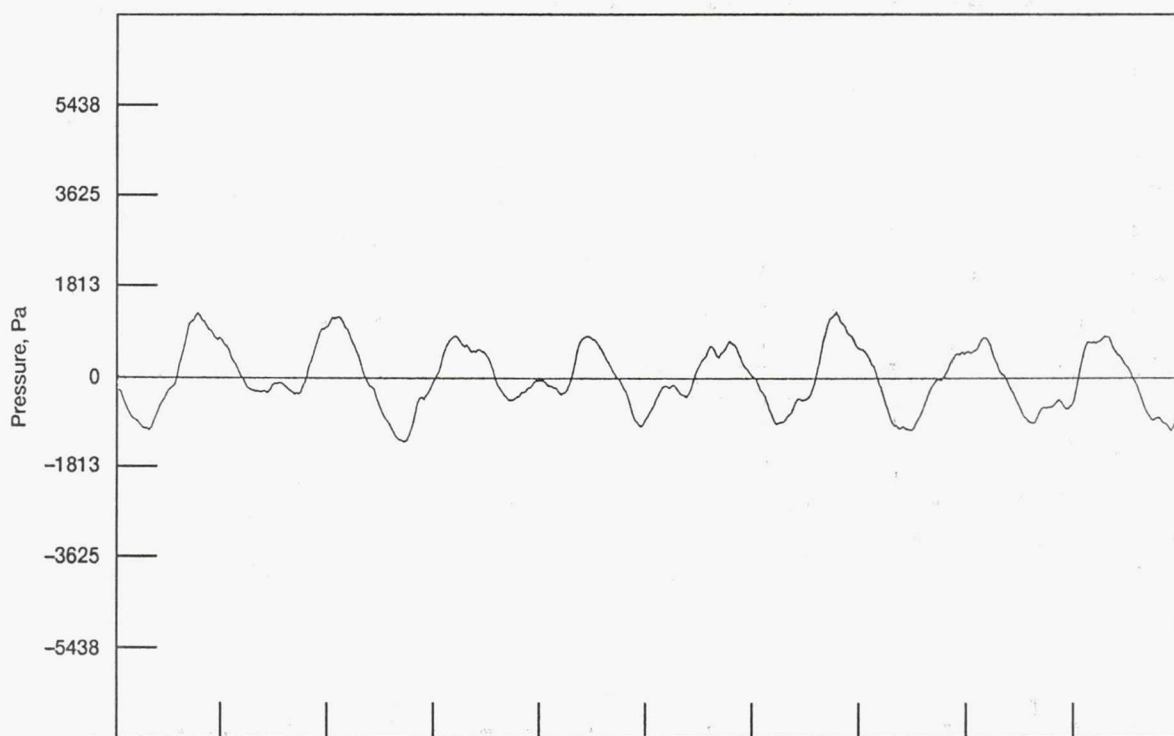


(c) Transducer 3.

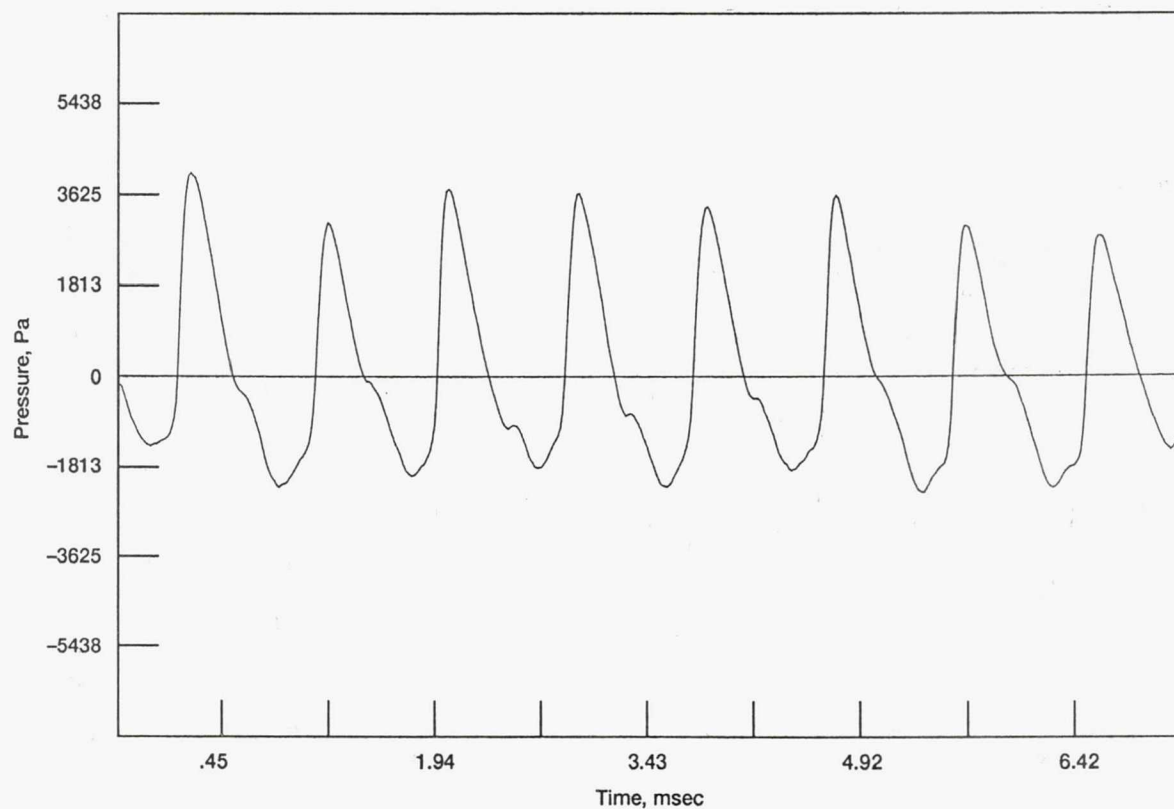


(d) Transducer 4.

Figure 7.—Continued.



(e) Transducer 5.

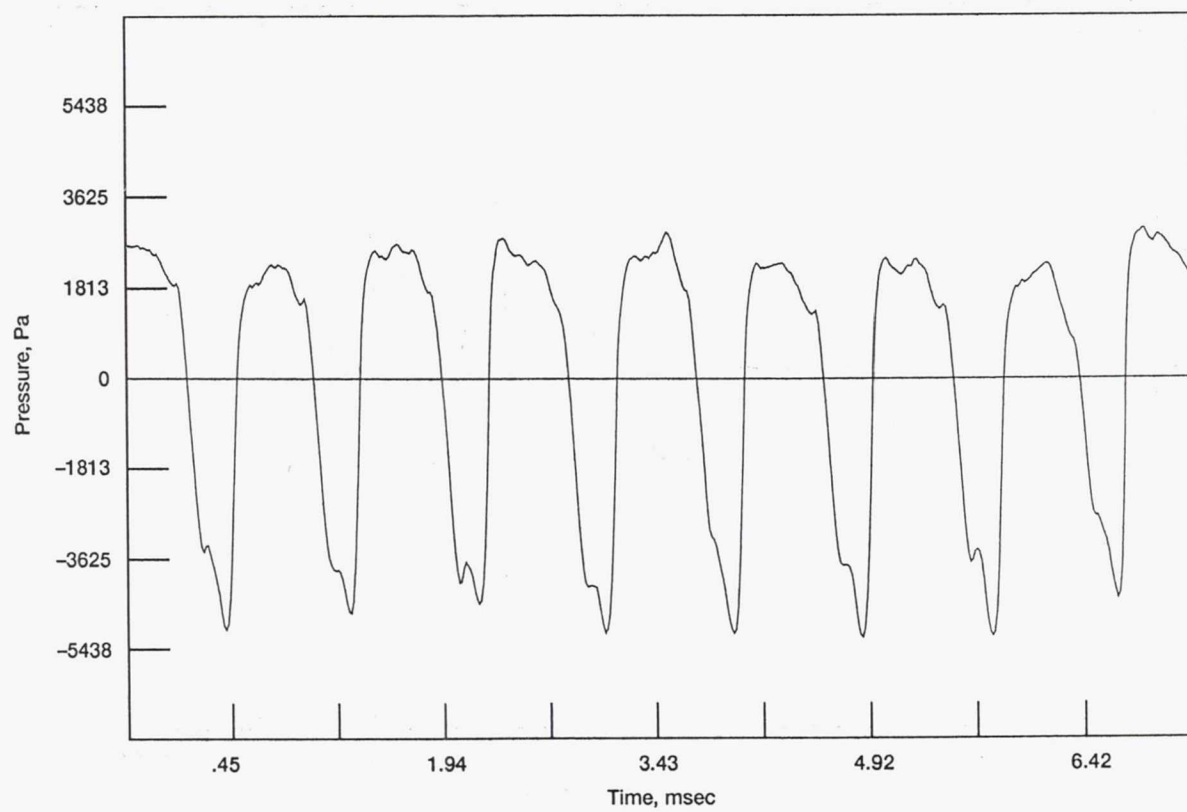


(f) Transducer 6.

Figure 7.—Continued.

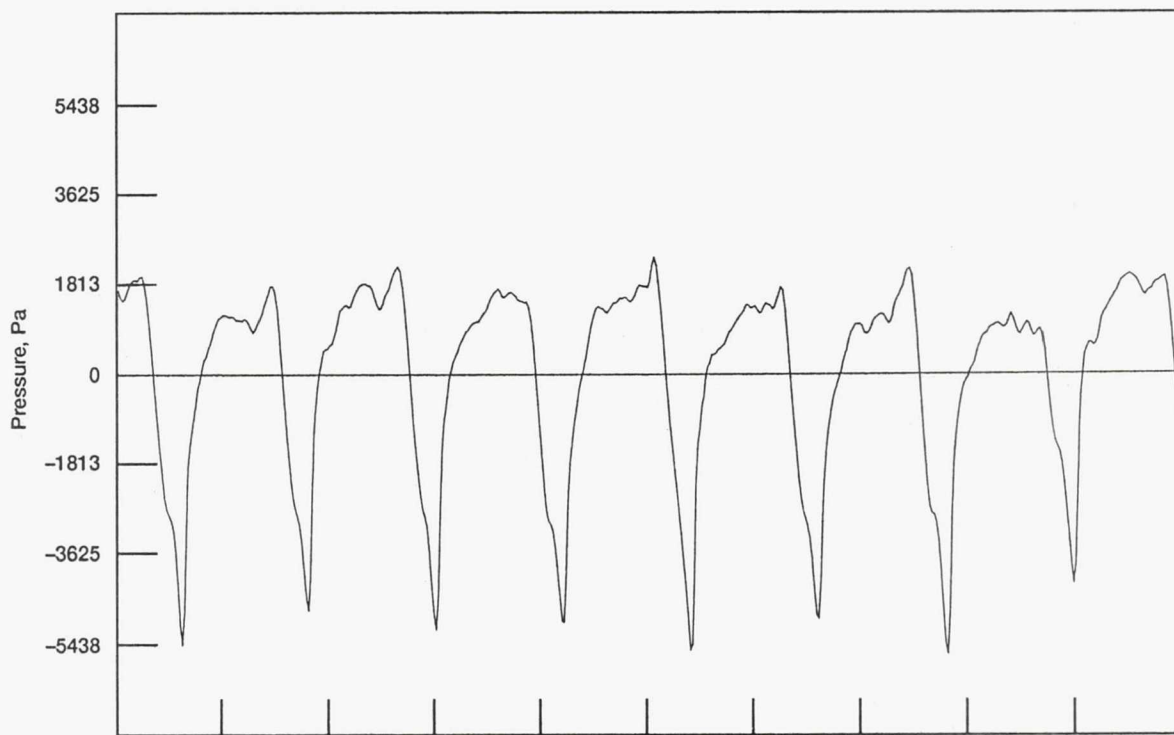


(g) Transducer 7.

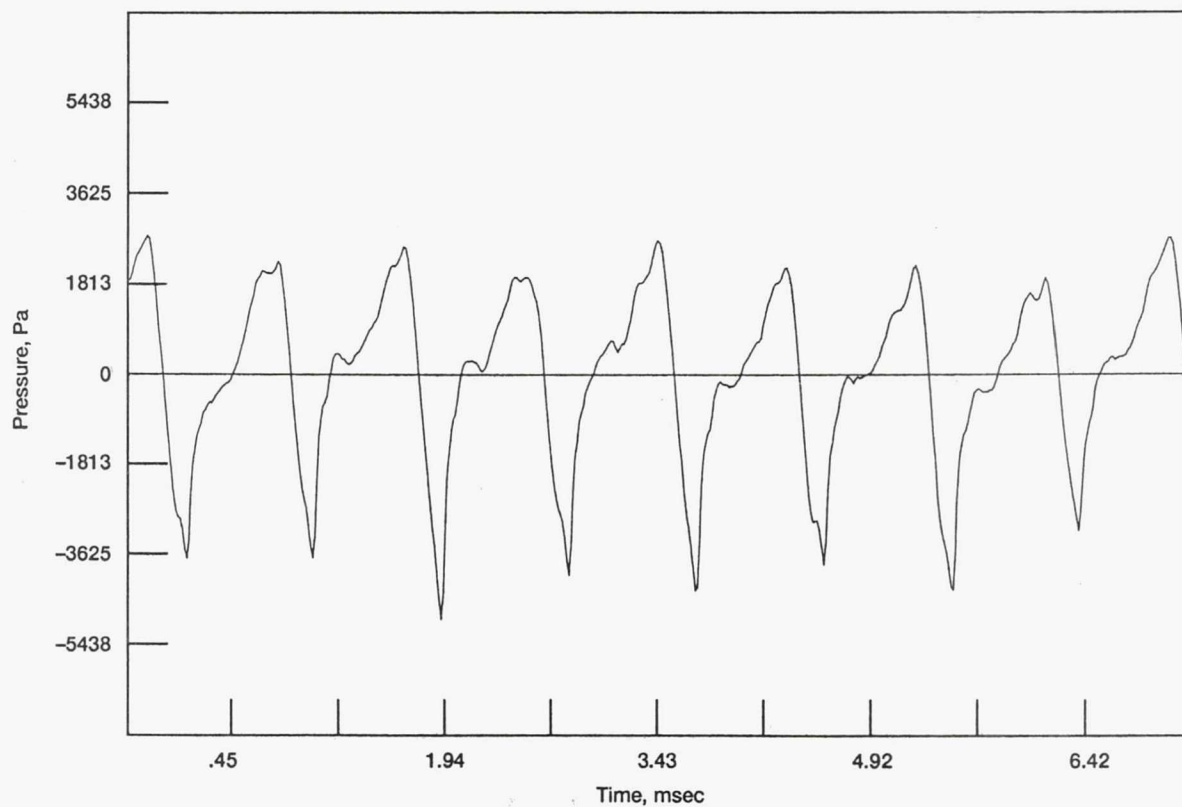


(h) Transducer 8.

Figure 7.—Continued.

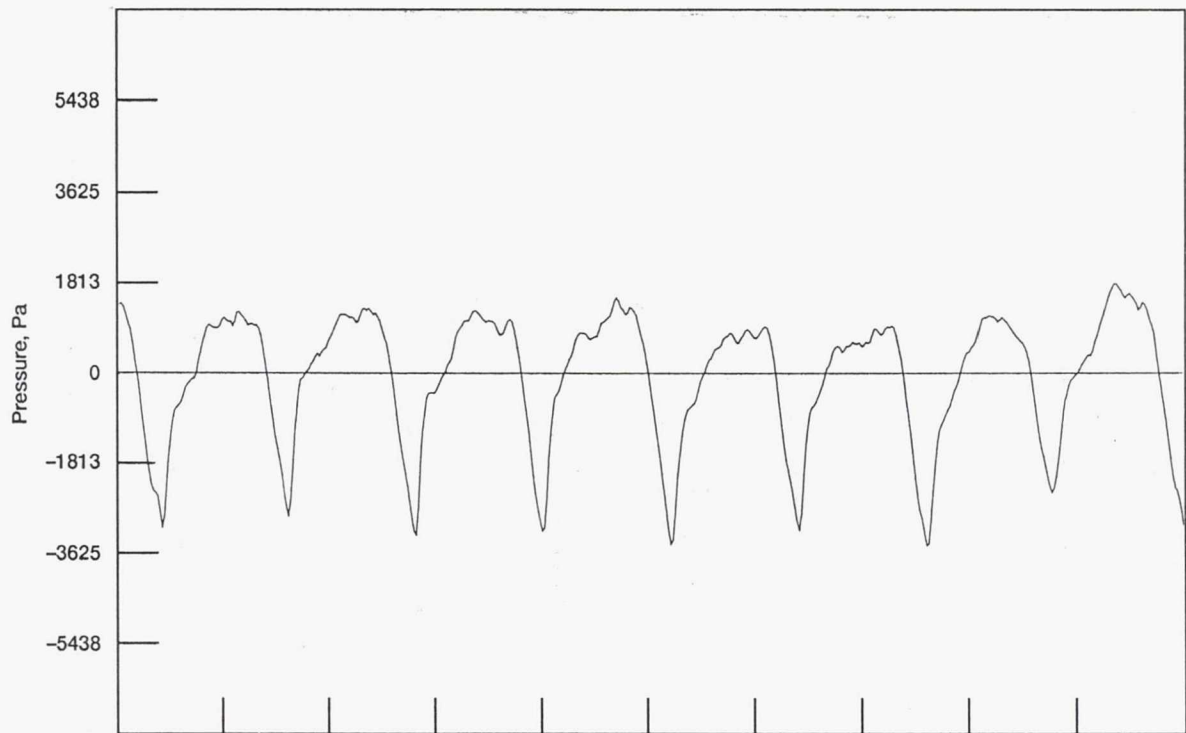


(i) Transducer 9.

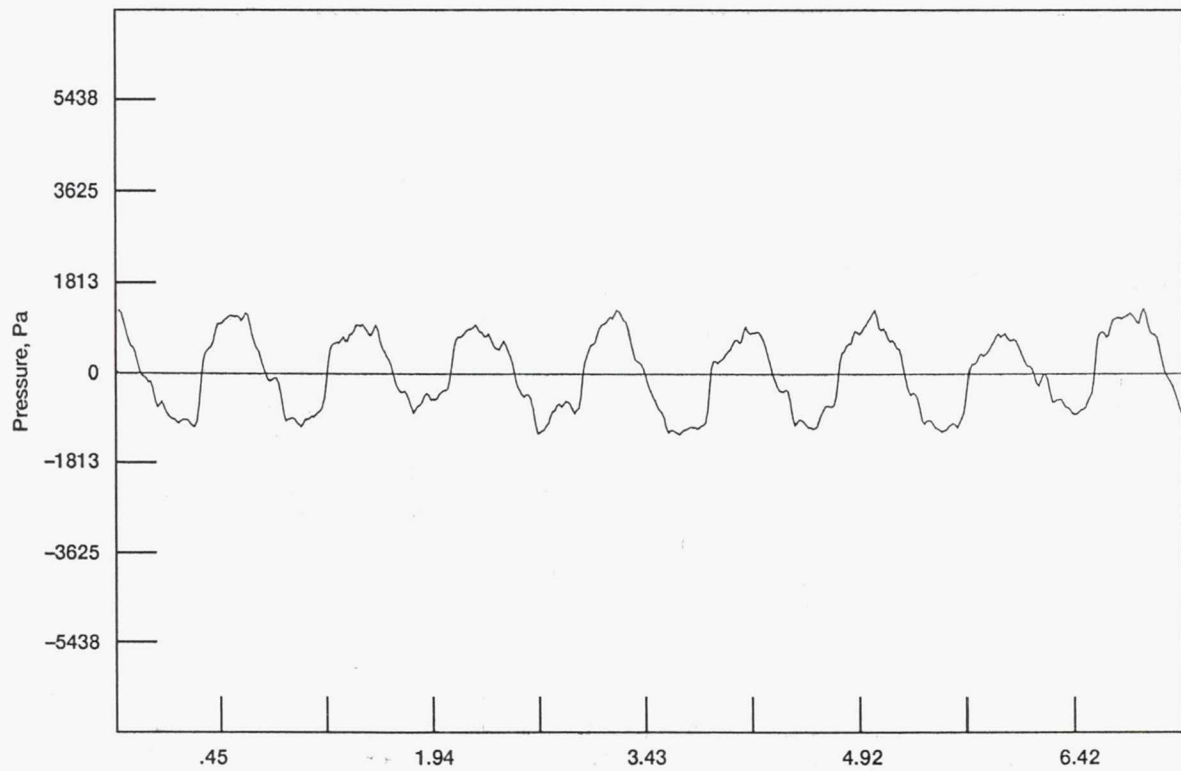


(j) Transducer 10.

Figure 7.—Continued.



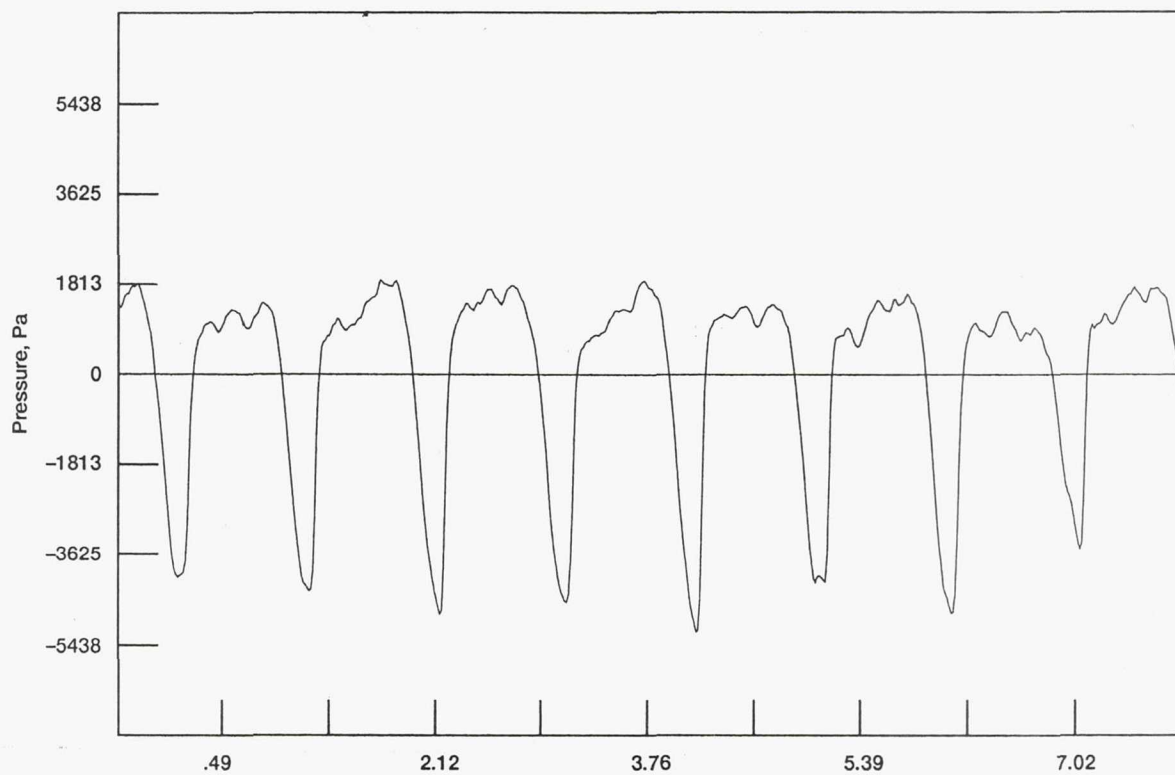
(k) Transducer 11.



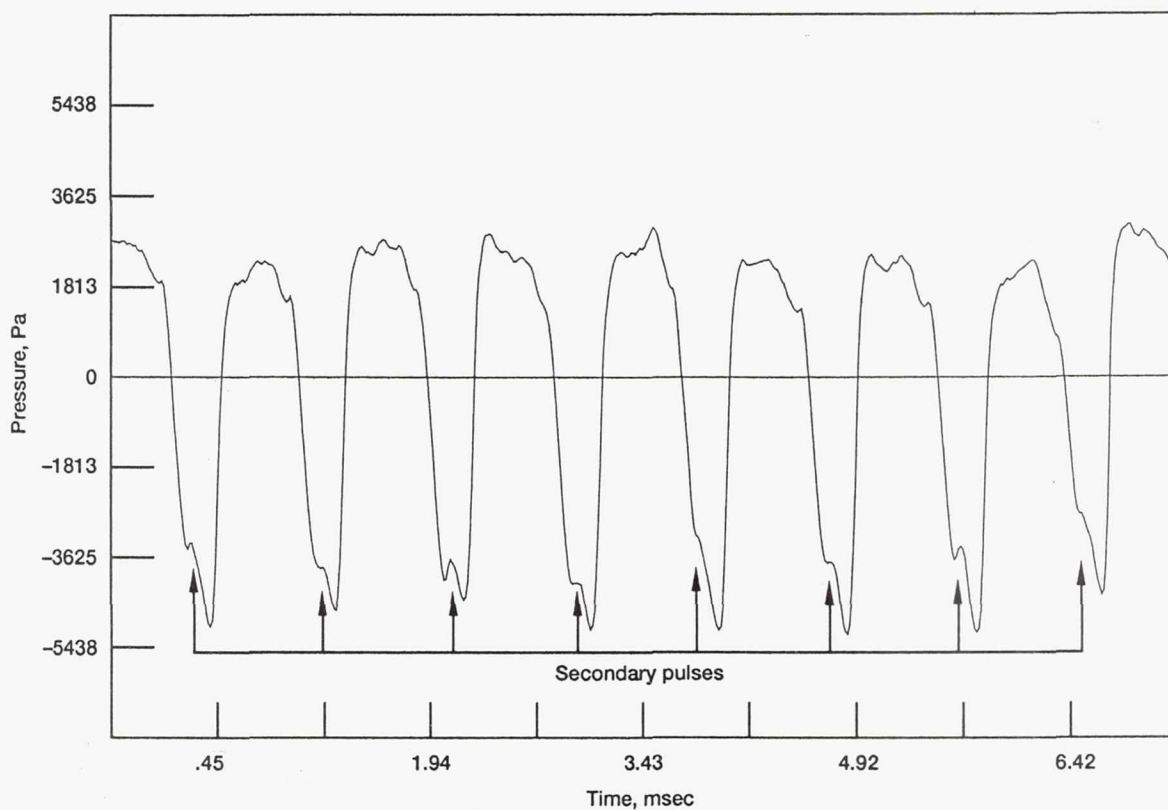
Time, msec

(l) Transducer 12.

Figure 7.—Concluded.



(a) $M = 0.72$, $M_{ht} = 1.03$; transducer No. 7.



(b) $M = 0.80$, $M_{ht} = 1.14$; transducer No. 8.

Figure 8.—Pressure-time histories at constant advance ratio of 3.06.

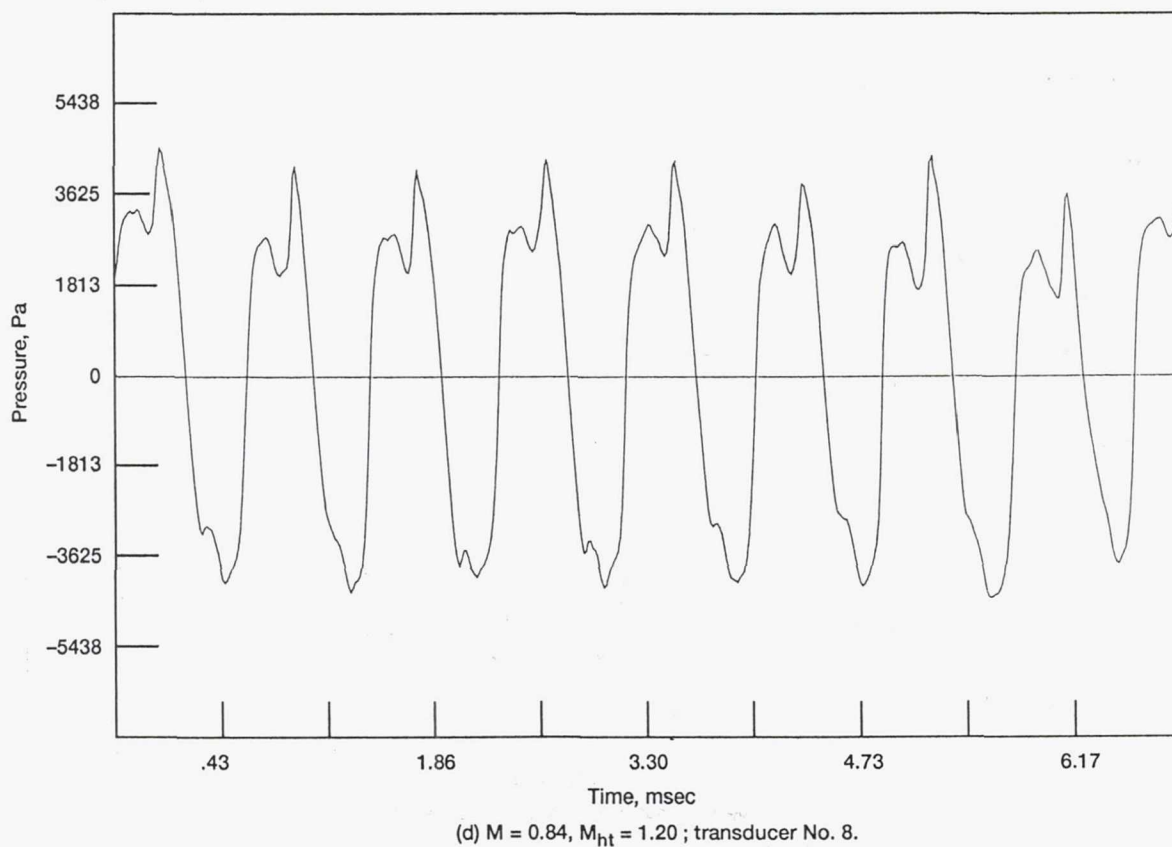
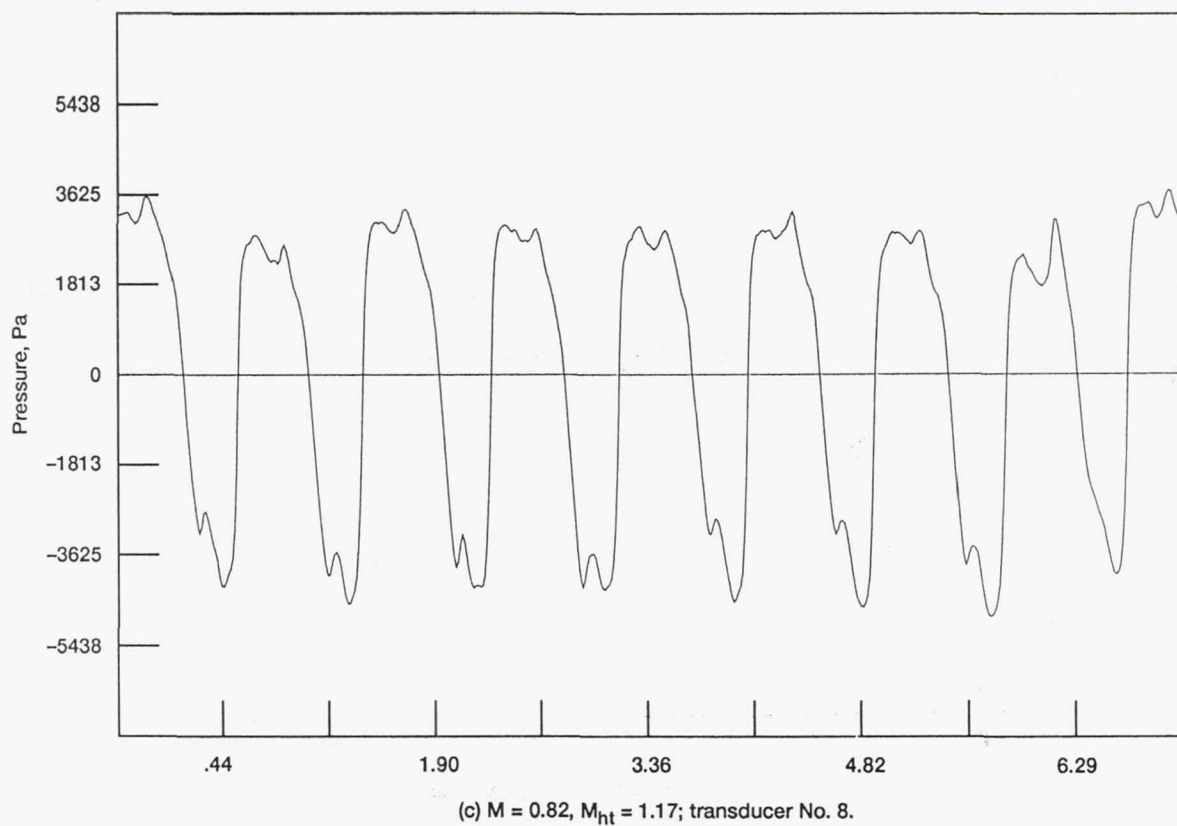
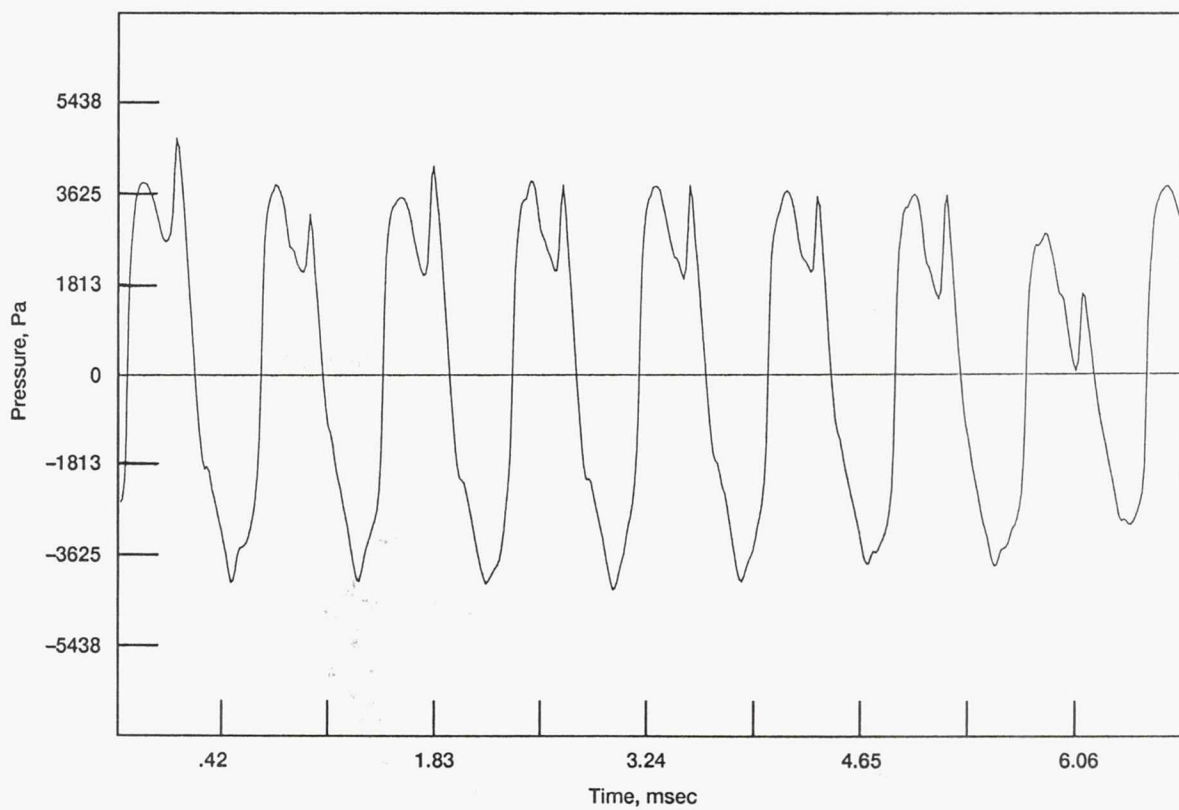
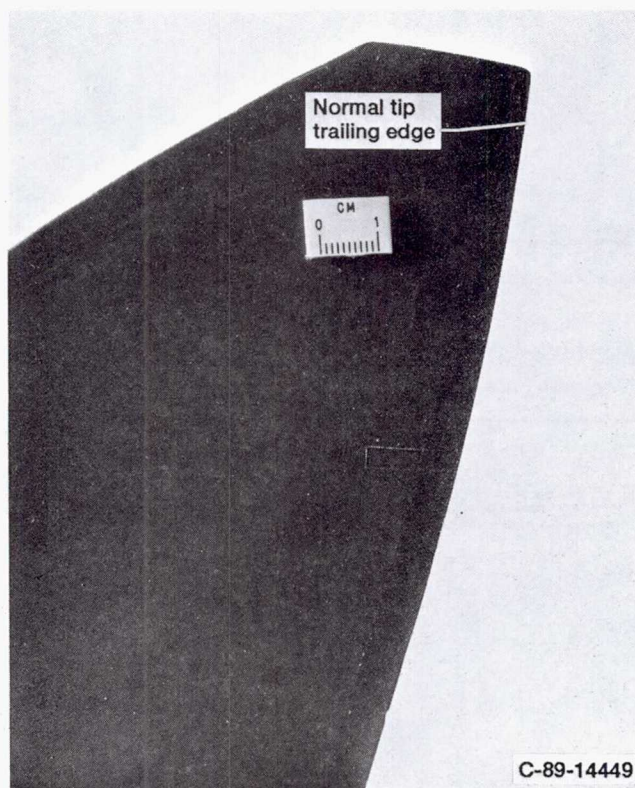


Figure 8.—Continued.

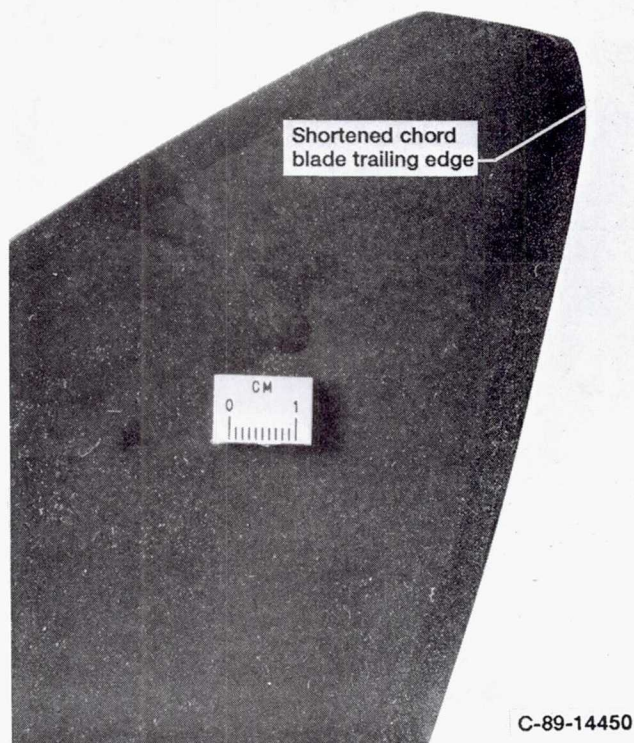


(e) $M = 0.86$, $M_{ht} = 1.23$; transducer No. 8.

Figure 8.—Concluded.

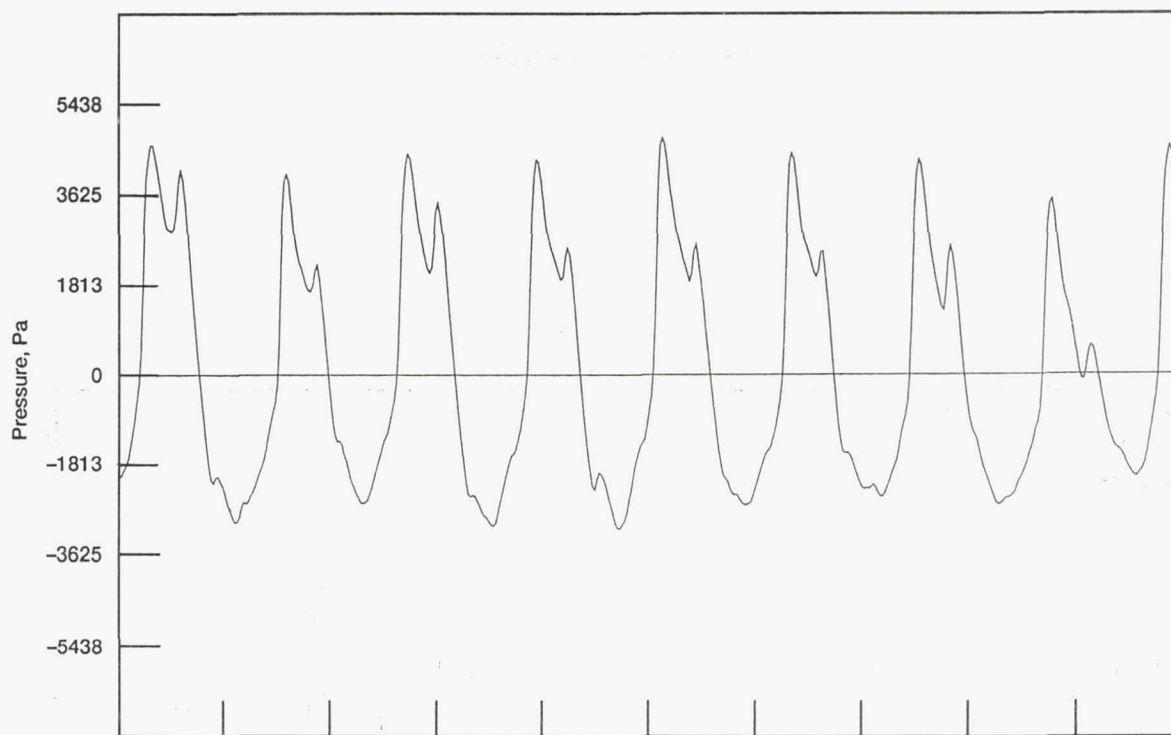


(a) Normal blade tip.

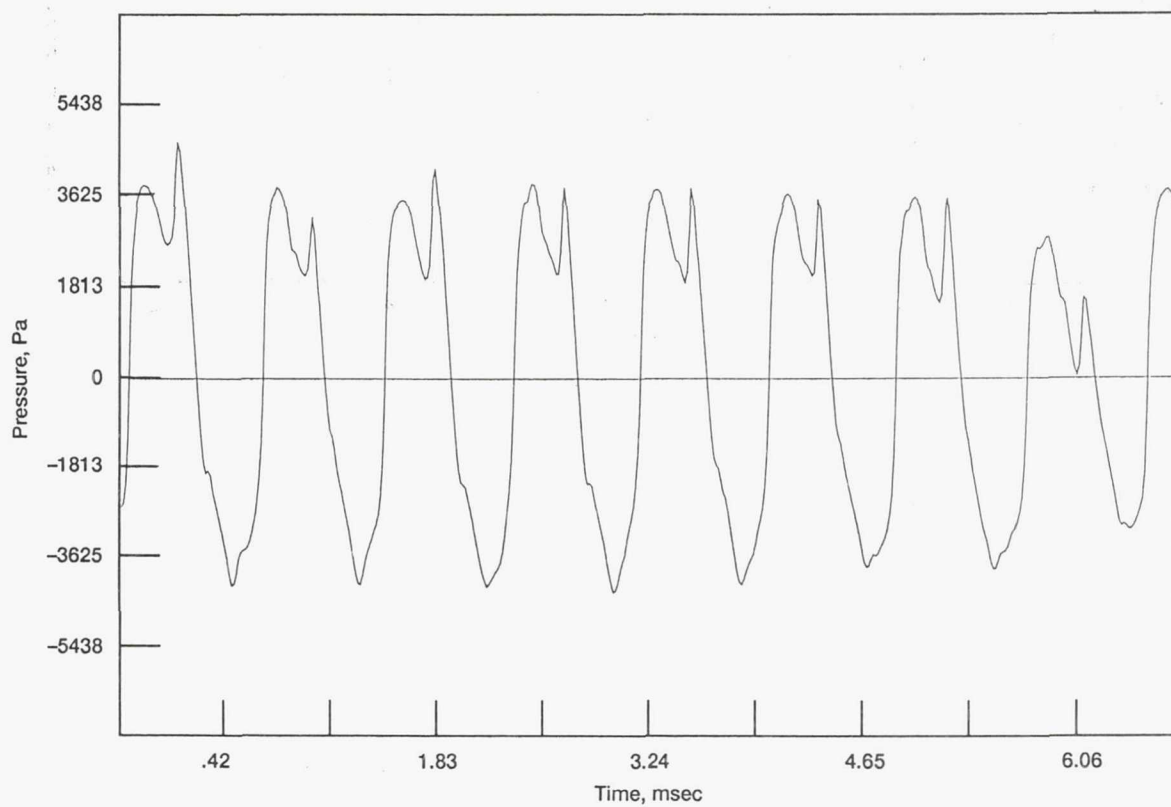


(b) Blade with shortened tip chord.

Figure 9.—Blade tip shape.

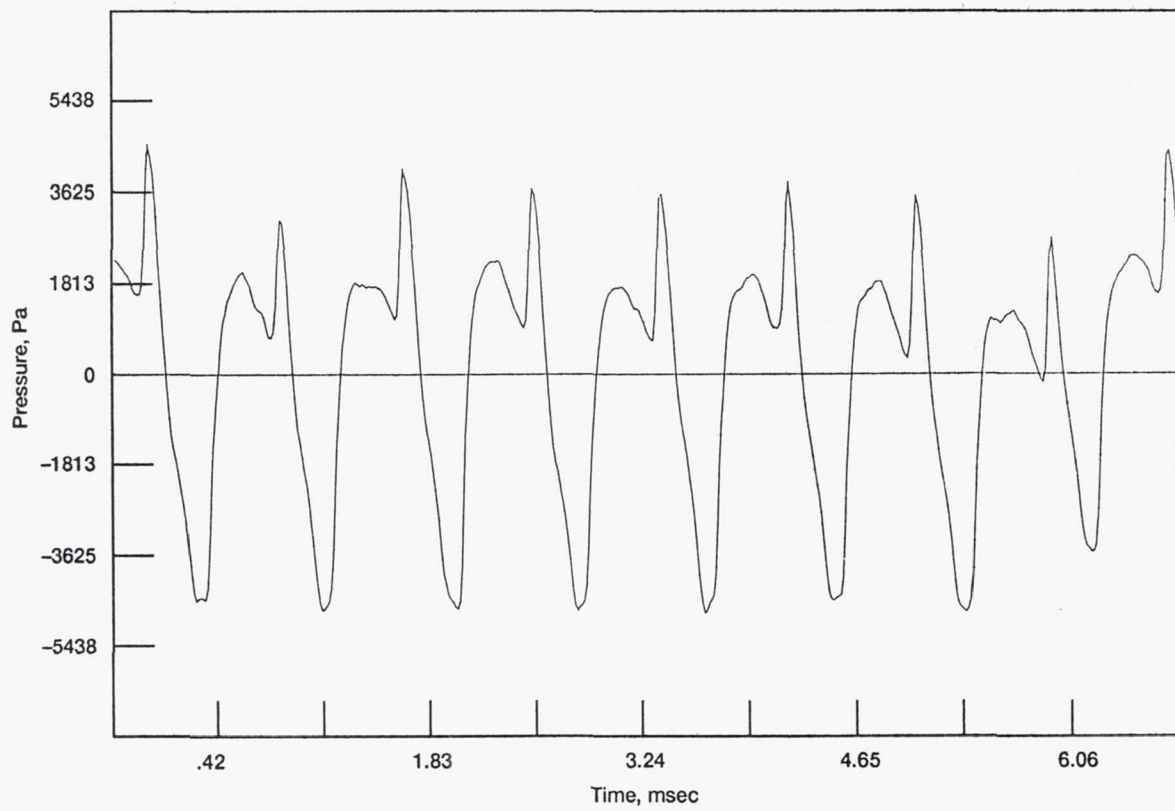


(a) Transducer 7.



(b) Transducer 8.

Figure 10.—Pressure-time histories at $M = 0.86$, $M_{ht} = 1.23$.



(c) Transducer 9.

Figure 10.—Concluded.

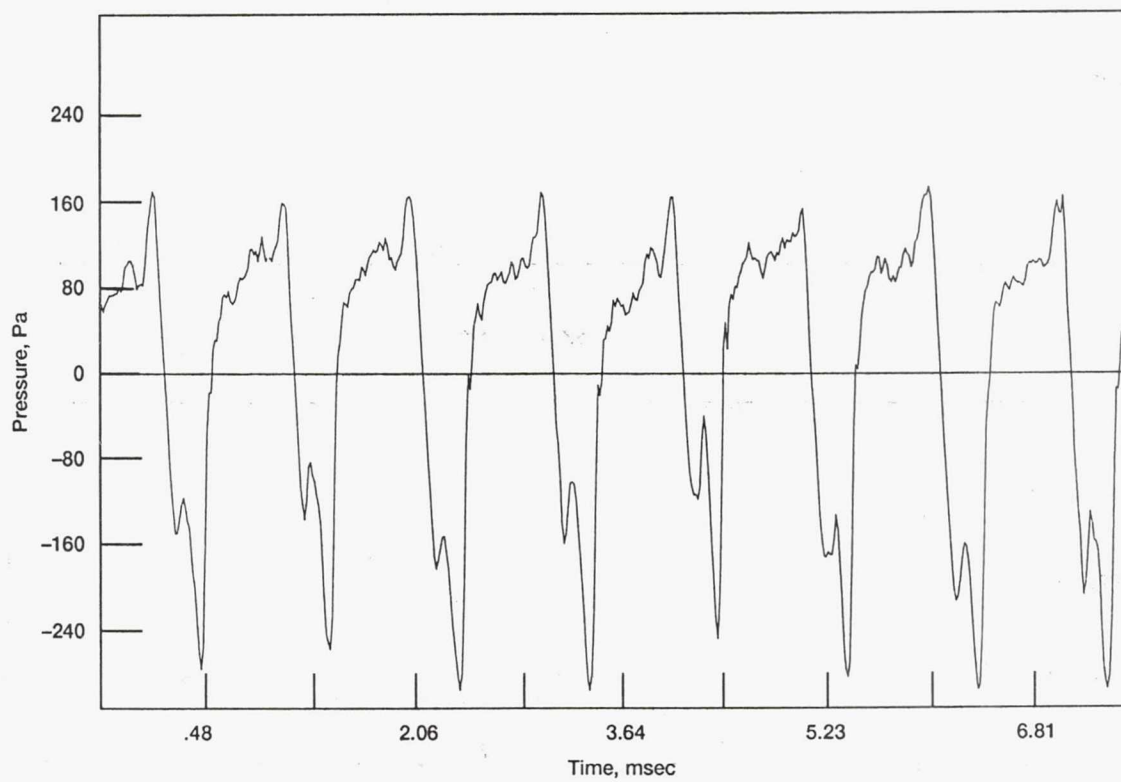


Figure 11.—Pressure-time history from SR-3 propeller on Jetstar airplane.

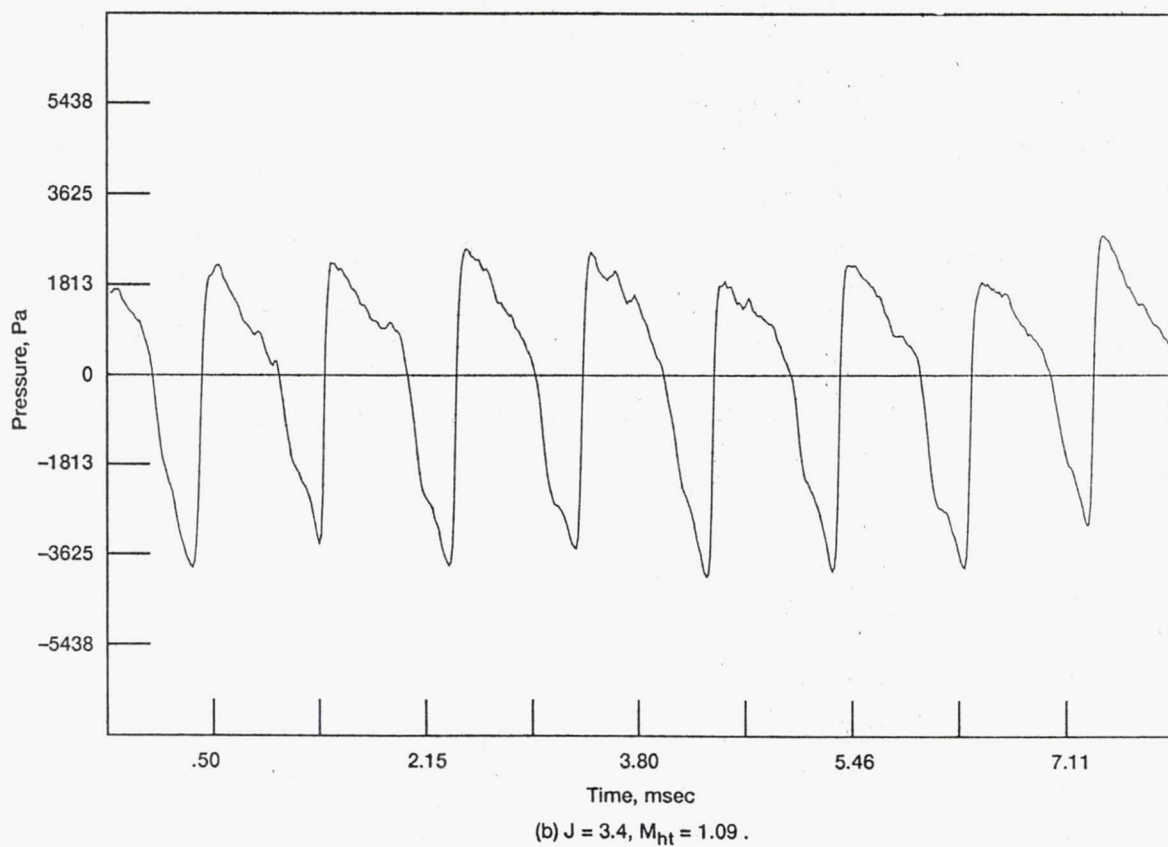
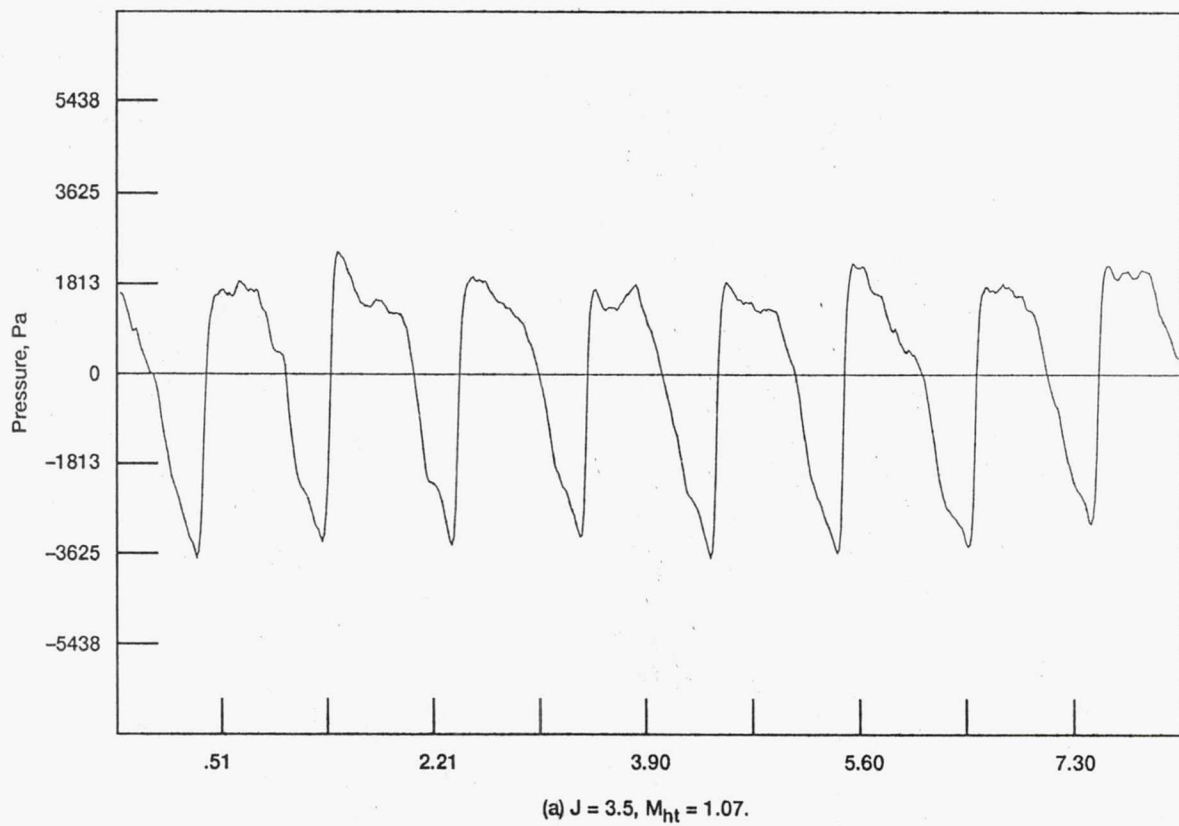
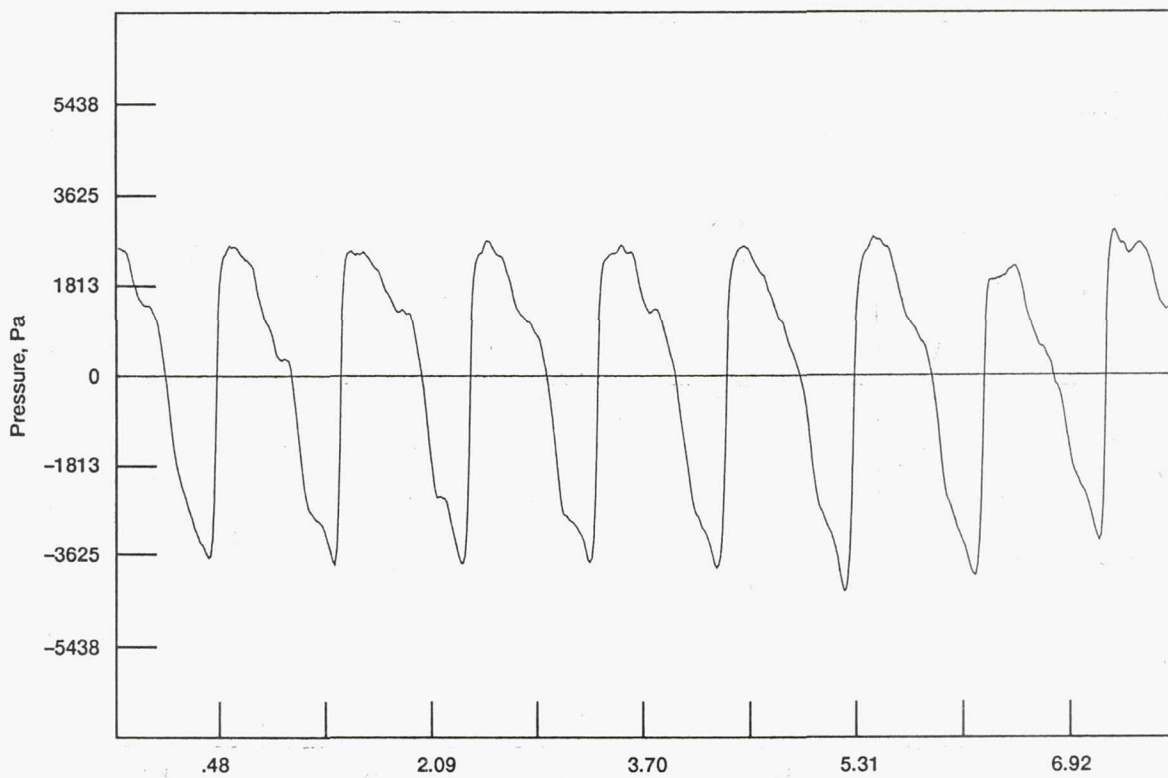
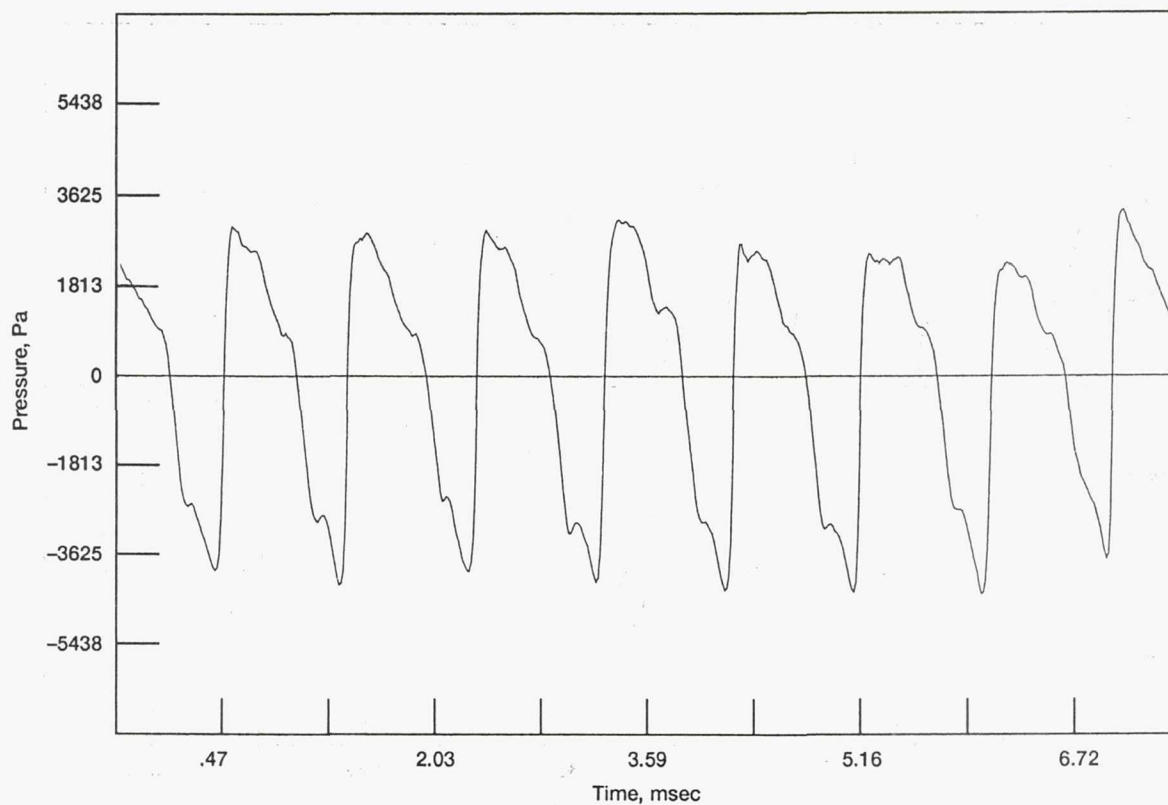


Figure 12.—Pressure-time histories at constant axial Mach number of 0.8.

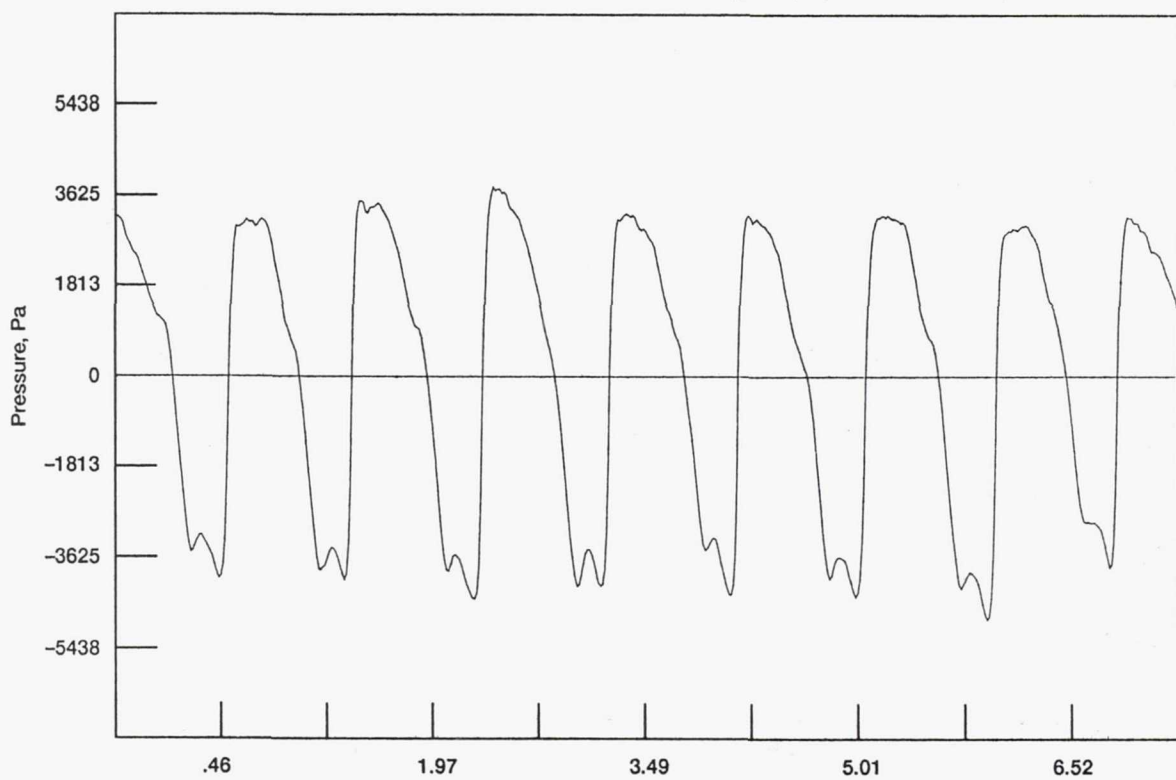


(c) $J = 3.3$, $M_{ht} = 1.10$.

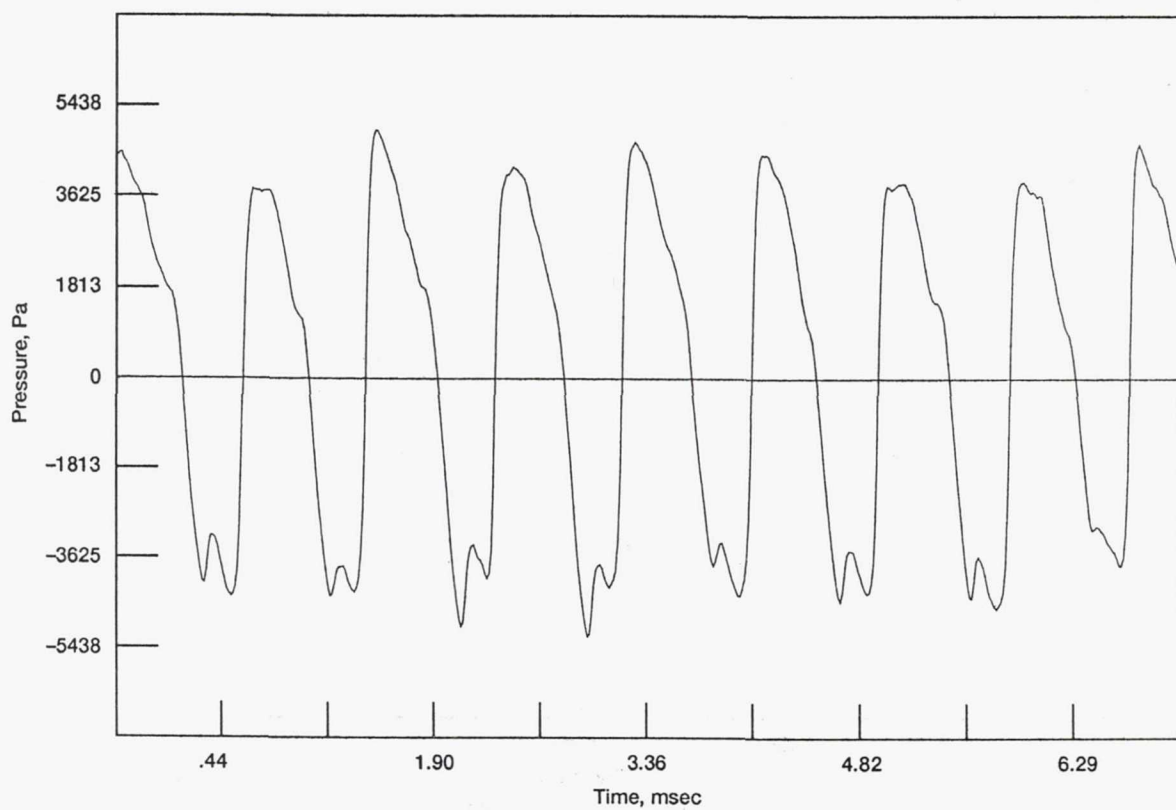


(d) $J = 3.20$, $M_{ht} = 1.12$.

Figure 12.—Continued.

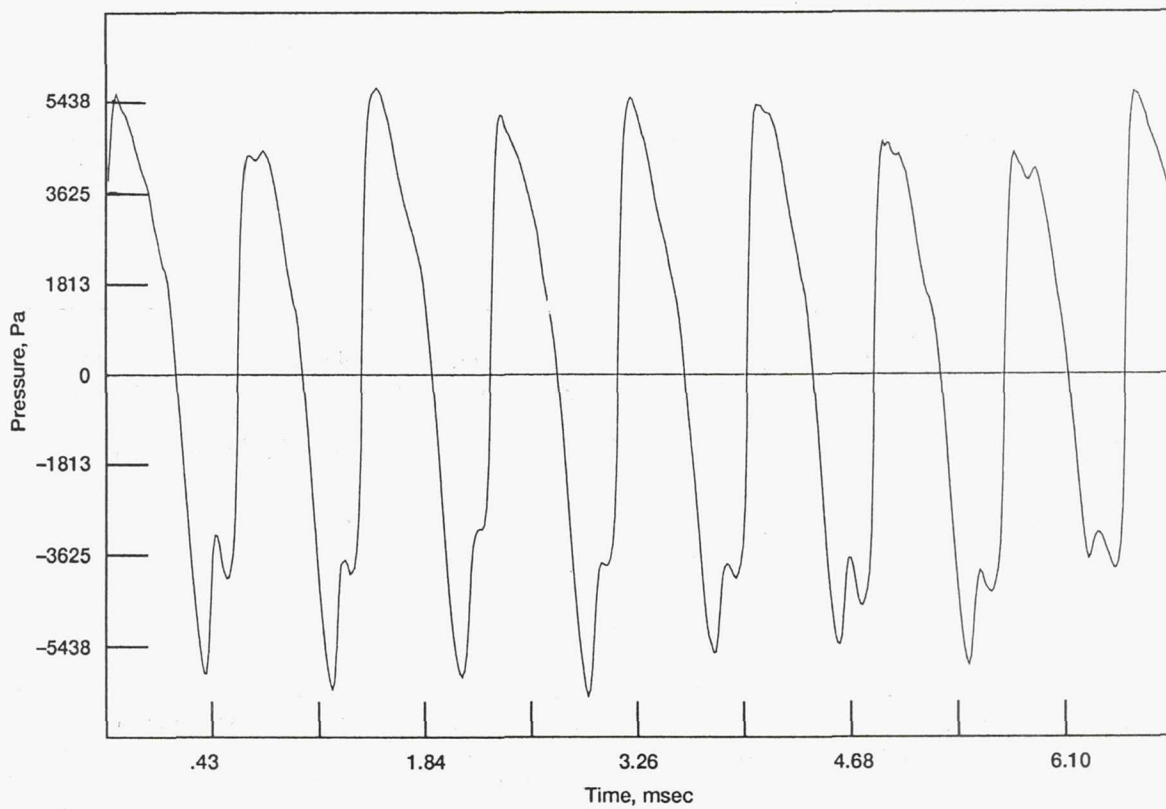


(e) $J = 3.10$, $M_{ht} = 1.13$.



(f) $J = 3.00$, $M_{ht} = 1.15$.

Figure 12.—Continued.



(g) $J = 2.90$, $M_{ht} = 1.17$.

Figure 12.—Concluded.

REPORT DOCUMENTATION PAGEForm Approved
OMB No. 0704-0188

Public reporting burden for this collection of information is estimated to average 1 hour per response, including the time for reviewing instructions, searching existing data sources, gathering and maintaining the data needed, and completing and reviewing the collection of information. Send comments regarding this burden estimate or any other aspect of this collection of information, including suggestions for reducing this burden, to Washington Headquarters Services, Directorate for Information Operations and Reports, 1215 Jefferson Davis Highway, Suite 1204, Arlington, VA 22202-4302, and to the Office of Management and Budget, Paperwork Reduction Project (0704-0188), Washington, DC 20503.

1. AGENCY USE ONLY (Leave blank)		2. REPORT DATE December 1991	3. REPORT TYPE AND DATES COVERED Technical Memorandum	
4. TITLE AND SUBTITLE Detailed Noise Measurements on the SR-7A Propeller: Tone Behavior With Helical Tip Mach Number			5. FUNDING NUMBERS WU - 535 - 03 - 10	
6. AUTHOR(S) James H. Dittmar and David G. Hall				
7. PERFORMING ORGANIZATION NAME(S) AND ADDRESS(ES) National Aeronautics and Space Administration Lewis Research Center Cleveland, Ohio 44135 - 3191			8. PERFORMING ORGANIZATION REPORT NUMBER E - 6519	
9. SPONSORING/MONITORING AGENCY NAMES(S) AND ADDRESS(ES) National Aeronautics and Space Administration Washington, D.C. 20546 - 0001			10. SPONSORING/MONITORING AGENCY REPORT NUMBER NASA TM - 105206	
11. SUPPLEMENTARY NOTES James H. Dittmar, NASA Lewis Research Center; David G. Hall, Sverdrup Technology, Inc., Lewis Research Center Group, 2001 Aerospace Parkway, Brook Park, Ohio 44142. Responsible person, James H. Dittmar, (216) 433 - 3921.				
12a. DISTRIBUTION/AVAILABILITY STATEMENT Unclassified - Unlimited Subject Category 71			12b. DISTRIBUTION CODE	
13. ABSTRACT (Maximum 200 words) Detailed noise measurements were taken on the SR-7A propeller to investigate the behavior of the noise with helical tip Mach number. Data sets taken at constant advance ratio and at constant axial Mach number both showed the noise to first rise with increasing helical tip Mach number and then to level off as the Mach number was increased further. This behavior was further investigated by obtaining detailed pressure-time histories of the data. The pressure-time histories indicate that a portion of the primary pressure pulse is progressively canceled by a secondary pulse which results in the noise leveling off as the helical tip Mach number is increased. This second pulse appears to originate on the same blade as the primary pulse and is in some way connected to the blade itself. This leaves open the possibility of redesigning the blade to improve the cancellation and thereby reduce the propeller noise.				
14. SUBJECT TERMS Propeller noise; Noise; Supersonic tip speed			15. NUMBER OF PAGES 30	
			16. PRICE CODE A03	
17. SECURITY CLASSIFICATION OF REPORT Unclassified	18. SECURITY CLASSIFICATION OF THIS PAGE Unclassified	19. SECURITY CLASSIFICATION OF ABSTRACT Unclassified	20. LIMITATION OF ABSTRACT	